AWARD NUMBER:

W81XWH-15-1-0024

TITLE: Modulation of Ocular Inflammation by Mesenchymal Stem Cells

PRINCIPAL INVESTIGATOR: Sunil Chauhan, DVM, PhD

CONTRACTING ORGANIZATION: Schepens Eye Research Institute

Boston, MA 02114

REPORT DATE: March 2017

TYPE OF REPORT: Final

PREPARED FOR: U.S. Army Medical Research and Materiel Command

Fort Detrick, Maryland 21702-5012

DISTRIBUTION STATEMENT: Approved for Public Release;
                                            Distribution Unlimited

The views, opinions and/or findings contained in this report are those of the author(s) and should not be construed as an official Department of the Army position, policy or decision unless so designated by other documentation.

REPORT DOCUMENTATION PAGE

1. REPORT DATE *(DD-MM-YYYY)*	2. REPORT TYPE	3. DATES COVERED *(From - To)*
March 2017	Final	24 Dec 2014 - 23 Dec 2016

4. TITLE AND SUBTITLE

Modulation of Ocular Inflammation by Mesenchymal Stem Cells

5a. CONTRACT NUMBER

5b. GRANT NUMBER
W81XWH-15-1-0024

5c. PROGRAM ELEMENT NUMBER

6. AUTHOR(S)
Sunil Chauhan
Afsaneh Amouzegar

Email: Sunil_Chauhan@meei.harvard.edu

5d. PROJECT NUMBER

5e. TASK NUMBER

5f. WORK UNIT NUMBER

7. PERFORMING ORGANIZATION NAME(S) AND ADDRESS(ES)

Schepens Eye Research Institute
20 Staniford Street
Boston, MA 02114-2508

8. PERFORMING ORGANIZATION REPORT

9. SPONSORING / MONITORING AGENCY NAME(S) AND ADDRESS(ES)

U.S. Army Medical Research and Materiel Command
Fort Detrick, Maryland 21702-5012

10. SPONSOR/MONITOR'S ACRONYM(S)

11. SPONSOR/MONITOR'S REPORT NUMBER(S)

12. DISTRIBUTION / AVAILABILITY STATEMENT
Approved for public release; distribution unlimited.

13. SUPPLEMENTARY NOTES

14. ABSTRACT:
Ocular injury and inflammations are commonly treated with non-specific anti-inflammatory drugs such as corticosteroids. These non-specific treatments typically target both pathogenic and regulatory cells of the immune system, and are associated with side effects such as infection, cataract and glaucoma. Thus, there is a pressing need for new immunomodulatory strategies that not only inhibit pathogenic immune cells, but also promote critical regulatory immune cells that promote immune quiescence, such as myeloid-derived suppressor cells (MDSC). Bone marrow-derived mesenchymal stem cells (BM-MSC) have shown promise in exerting immunomodulatory functions, and present a novel and potentially effective alternative to the current non-specific immunosuppressive therapies. The goal of this project is to investigate the mechanisms by which BM-MSC modulate maturation and differentiation of immature myeloid progenitor cells into MDSC (away from pathogenic macrophages) to control ocular inflammation. We anticipate that these investigations will identify critical immunomodulatory factors which may be used to design novel, targeted strategies for treating eye injury and inflammation.

15. SUBJECT TERMS   Nothing listed

16. SECURITY CLASSIFICATION OF:			17. LIMITATION OF ABSTRACT	18. NUMBER OF PAGES	19a. NAME OF RESPONSIBLE PERSON USAMRMC
a. REPORT U	**b. ABSTRACT** U	**c. THIS PAGE** U	UU	61	19b. TELEPHONE NUMBER

Table of Contents

1. INTRODUCTION

Bone marrow derived mesenchymal stem cells (BM-MSC) are a heterogeneous population of stromal cells that have considerable regenerative and immunomodulatory properties. The immunosuppressive effect of BM-MSC on pathogenic immune cells including effector T cells, macrophages and dendritic cells has been established. Studies have shown that BM-MSC inhibit generation, migration and function of macrophages. Preliminary data from our laboratory has shown that during ocular inflammation, BM-MSC are capable of promoting the differentiation of immature myeloid granulocyte-macrophage progenitors (GMP) into regulatory immune cells such as myeloid derived suppressor cells (MDSC) that could counter the effect of inflammatory macrophages. MDSC are a group of highly immunoregulatory cells that are categorized into monocytic MDSC ($CD11b^+$ $Ly6C^{hi}$ $Ly6G^-$) and granulocytic MDSC ($CD11b^+$ $Ly6C^{lo}$ $Ly6G^+$) based on their phenotype. Monocytic subpopulations of MDSC have significant immunosuppressive activity and their immunomodulatory role in tumors, transplant rejection and chronic inflammatory diseases of the eye has been established. The goal of this project is to investigate the mechanisms by which BM-MSC modulate maturation and differentiation of GMP into MDSC to control ocular inflammation.

2. KEYWORDS: ocular inflammation, mesenchymal stem cells, MDSC

3. ACCOMPLISHMENTS

●What were the major goals of the project?

Task #1: Determine mesenchymal stem cell (BM-MSC)-mediated immature myeloid progenitor (GMP) cell differentiation into monocytic versus granulocytic myeloid-derived suppressor cells (MDSC)
<div align="right">(Jan 2015 – Aug 2015)</div>

Task #2: Define critical factors expressed by BMMSC that promote GMP differentiation into MDSC
<div align="right">(Sep 2015 – Apr 2016)</div>

Task #3: Assess effect of in vivo administration of BMSC on MDSC frequency and ocular inflammation
<div align="right">(May 2016 – Dec 2016)</div>

●**What was accomplished under these goals?**

Task #1: Determine BM-MSC-mediated GMP differentiation into monocytic versus granulocytic MDSC   **(Jan 2015 – Aug 2015)**

Local IACUC Approval   (100% completion)   (Jan 2015 – Feb 2015)
1) Major activities: A postdoctoral research fellow (Dr. Afsaneh Amouzegar, MD) has been hired to perform experiments on this project. A personnel amendment for Dr. Amouzegar to animal protocol was submitted to IACUC and ACURO.
2) Specific objectives: ACURO approval, and Dr. Amouzegar's animal handling training (both online and hands-on) by the Animal Facility Staff and experienced laboratory members.
3) Significant results: Both ACURO approval and Dr. Amouzegar's training are completed.

Subaim 1.A. Co-culture bone marrow-derived CD14^{+}CD11b$^{-/lo}$ GMP with BM-MSC
                        (100% completion)   (Mar 2015 – May 2015)
1) Major activities: Determine BM-MSC-mediated GMP differentiation into MDSC
2) Specific objectives: Co-culture of flow cytometry (FACS) based sorted CD14^{+}CD11b$^{-/lo}$ GMP cells from the bone marrow of C57BL/6 mice with in vitro cultured BM-MSC.
3) Significant results: Frequencies of CD14^{+}CD11b$^{-/lo}$ GMP cells were determined in bone marrow, spleen, and cervical lymph node of C57BL/6 mouse (**Figure 1**). GMPs were characterized for the expression of progenitor markers, CD34, c-Kit, FcγRII/III and maturation markers, CD11b, Ly6G and Ly6C (**Figure 2**). Bone marrow (from femurs) of euthanized C57BL/6 mice was harvested, and single cell suspension was stained with CD14-FITC and CD11b-PE/Cy5 monoclonal antibodies in sterile conditions. Then, using FACS sorting (MoFlo cell sorter, Dako Cytomation), a purified population of immature CD14^{+}CD11b$^{-/lo}$ GMP cells were freshly isolated. BM-MSC harvested from bone marrow from wild type C57BL6 mice were cultured in vitro. BM-MSC (5x10^5 cells) were co-cultured with GMP (1x10^6 cells) in the presence of pro-inflammatory cytokine IFNγ (100 ng/mL). After 72 hours, cultures were terminated and cells were immunostained with CD11b and Ly6G mAbs for multicolor flow cytometry to investigate the expression of CD11b (maturation marker expressed by macrophages) and Ly6G (maturation marker for granulocytes, such as neutrophils). As shown in **Figure 3**, with the addition of IFNγ, GMPs upregulate the expression of CD11b and Ly6G. However, in the presence of BM-MSCs in the inflammatory environment, there was a significant decrease in the expression levels of CD11b and Ly6G. These findings suggest that BM-MSC suppress GMP differentiation in the inflammatory environment. Furthermore, our results strongly suggest that in the presence of BM-MSCs, GMPs do not differentiate into MDCs and are rather kept in an undifferentiated state.
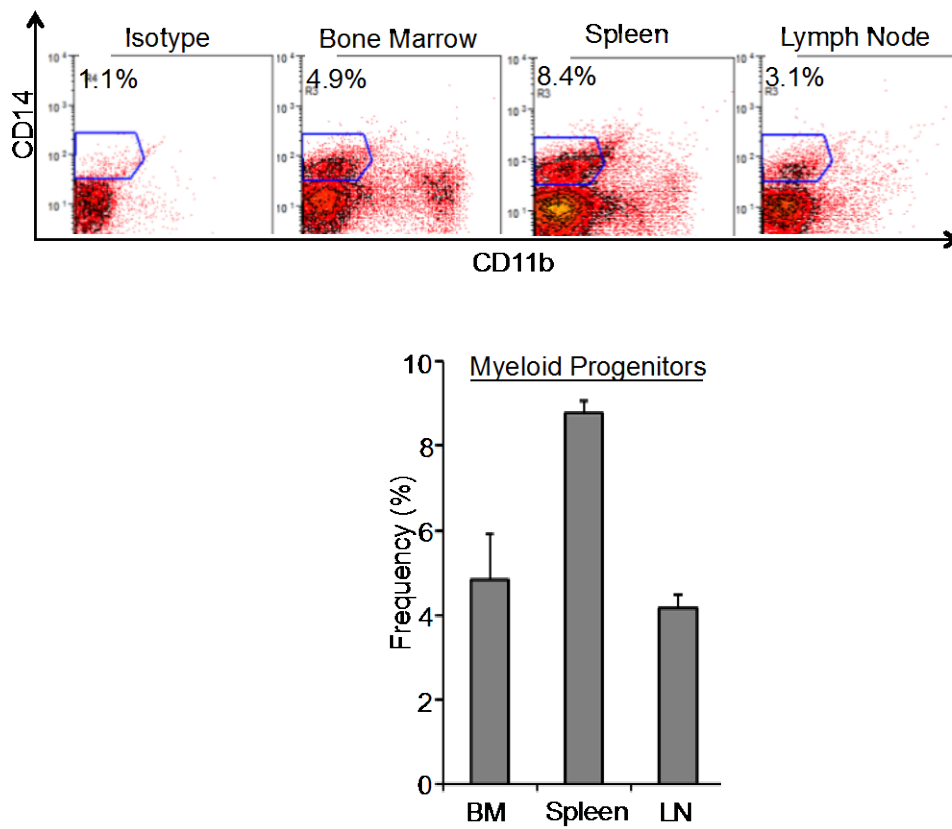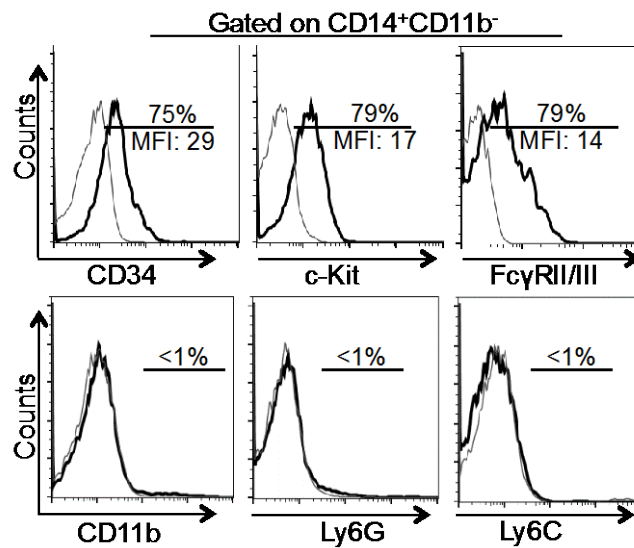
Figure 1. **Frequencies of GMPs in different tissues.**

Figure 2. **Phenotypic characterization of GMPs.** Surface expression of progenitor markers, CD34, c-Kit and FcγRII/III, and maturation markers, CD11b, Ly6G and Ly6C by GMPs.
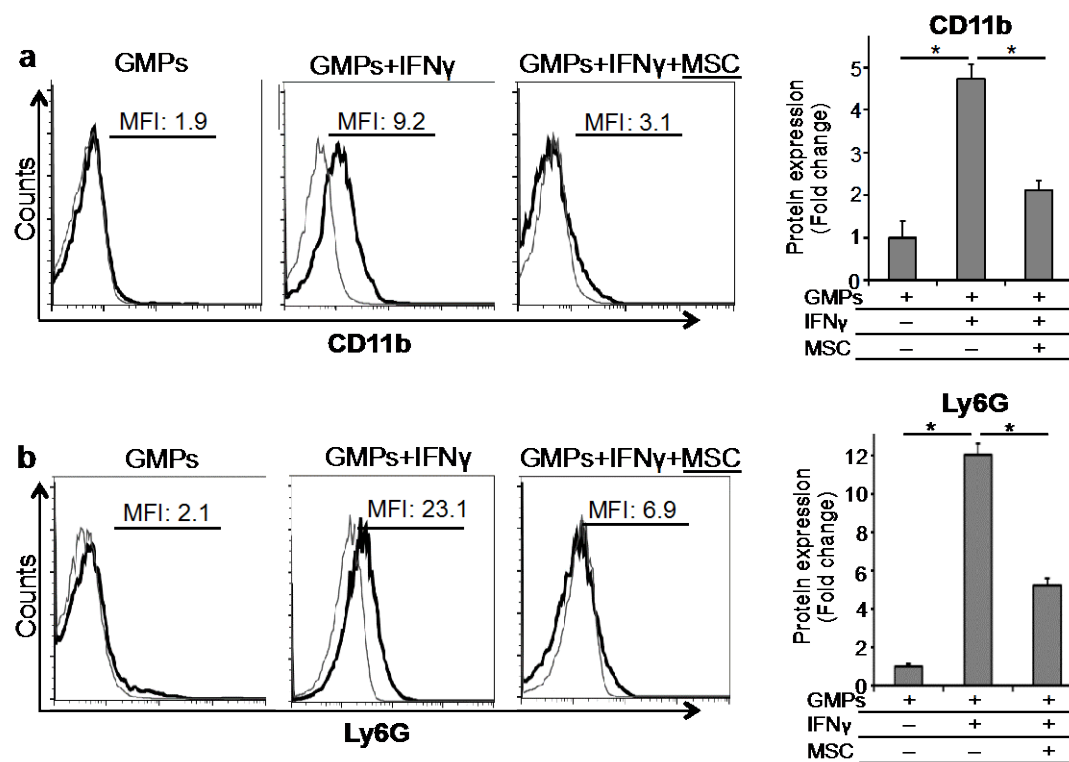
Figure 3. BM-MSC prevent GMP acquisition of **(a)** CD11b and **(b)** Ly6G maturation markers in the inflammatory environment in vitro.

Subaim 1.B. Co-culture corneal CD14$^+$CD11b$^{-/lo}$ GMP with BM-MSC

                        (100% completion)   **(June 2015 – August 2015)**

1) Major activities: determine BM-MSC-mediated corneal GMP differentiation into MDSCs

2) Specific objectives: determination of frequencies of GMPs in normal cornea using flow cytometry and immunohistochemistry; co-culture of flow cytometry (FACS) based sorted CD14$^+$CD11b$^{-/lo}$ GMP cells from the cornea of C57BL/6 mice with invitro cultured BM-MSC.

3) Significant results: Cornea of euthanized C57BL/6 mice was harvested and single cell suspension was stained with CD14-FITC, CD11b-PE/Cy5 and CD34-PE monoclonal antibodies for multicolor flow cytometry to determine the frequencies of CD34$^+$CD14$^+$CD11b$^-$ GMPs in normal cornea. Corneal whole mounts were also stained with CD14-FITC and CD11b-PE monoclonal antibodies and visualized using a confocal microscope (**Figure 4**). In order to investigate the effect of BM-MSC on corneal GMP differentiation, corneas from C57BL/6 mice were enzymatically digested and after preparing single cell suspension, a purified population of immature CD14$^+$CD11b$^{-/lo}$ GMP cells were freshly isolated using FACS sorting. BM-MSCs (2.5x10^4 cells) were co-cultured with corneal GMPs (5x10^4 cells) in the presence of pro-inflammatory cytokine IFNγ (100 ng/mL). After 72 hours, cultures were terminated and cells were immunostained for CD11b surface marker. As shown in **Figure 5**, in the presence of IFNγ approximately 12% of corneal GMPs acquired the CD11b maturation marker. However, with the addition of BM-MSC in the culture, there was a significant decrease in the frequencies of CD11b$^+$ cells, with only 1.5% of cells acquiring the surface marker. Similar to our previous findings, these results

strongly suggest that in the presence of BM-MSCs, GMPs do not differentiate into MDSCs and are maintained in an undifferentiated state.
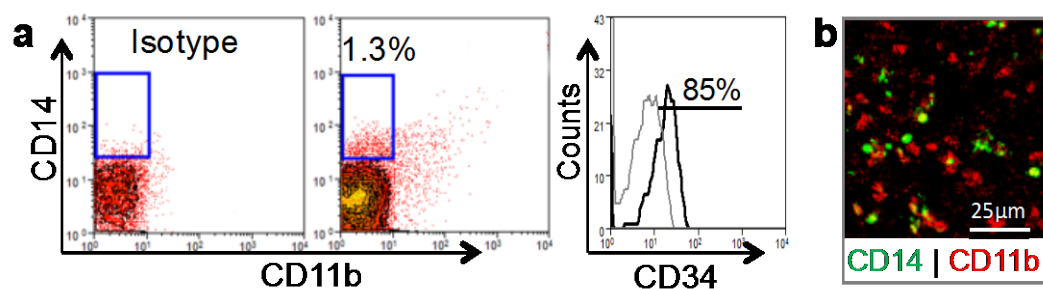

Figure 4. (a) Frequencies of $CD34^+$ $CD14^+$ $CD11b^{-/lo}$ GMPs in the cornea. **(b)** Confocal microscopy image ($\times$20) of corneal whole mount confirming the presence of $CD14^+$ $CD11b^-$ cells in the peripheral corneal stroma.
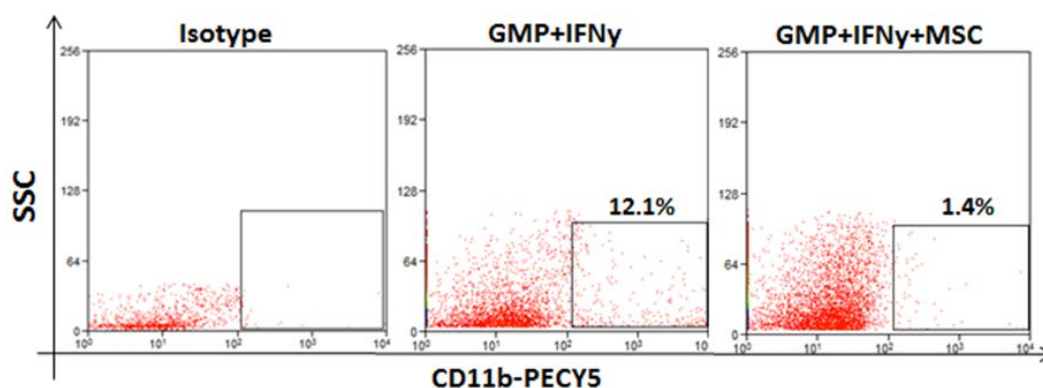

Figure 5. Corneal GMP acquisition of CD11b surface marker. BM-MSCs prevent acquisition of CD11b maturation marker by corneal GMPs in the inflammatory environment.

Task #2: Define critical factors expressed by BM-MSC that promote GMP differentiation into MDSC   **(September 2015-April 2016)**

Subaim 2.A. Define critical factors expressed by BM-MSC that promote GMP differentiation into MDSC
                              (100% completion)   (September 2015 – December 2015)
1) **Major activities**: determine mechanism of BM-MSC mediated suppression of GMP differentiation
2) **Specific objectives**: Determination of the mechanism by which BM-MSC suppress GMP differentiation and whether this effect is contact dependent or through secretion of soluble factors
3) **Significant results**: Bone marrow (from femurs) of euthanized C57BL/6 mice was harvested, and single cell suspension was stained with CD14-FITC and CD11b-PE/Cy5 monoclonal antibodies in sterile conditions. Then, using FACS sorting (MoFlo cell sorter, Dako Cytomation), a purified

population of immature $CD14^+CD11b^{-/lo}$ GMP cells were freshly isolated. BM-MSC harvested from bone marrow from wild type C57BL6 mice were cultured in vitro. BM-MSC (5x10^5 cells) were co-cultured with GMPs (1x10^6 cells) either directly or in the presence of Transwell polycarbonate membrane cell culture inserts (indirectly) in the presence of pro-inflammatory cytokine IFNγ (100 ng/mL). After 72 hours, cultures were terminated and cells were immunostained with CD11b mAb for multicolor flow cytometry to investigate the expression of CD11b differentiation marker. As shown in **Figure 6**, BM-MSC cultured in direct contact with GMPs suppressed GMP acquisition of CD11b, while in the presence of Transwell, BM-MSC did not have an inhibitory effect on differentiation of GMPs. This observation suggests that the immunomodulatory effect of BM-MSC on GMP is primarily contact-dependent and secretion of MSC-derived cytokines that were hypothesized to facilitate GMP differentiation into monocytic cells is not the primary mechanism by which BM-MSC modulate GMP differentiation.
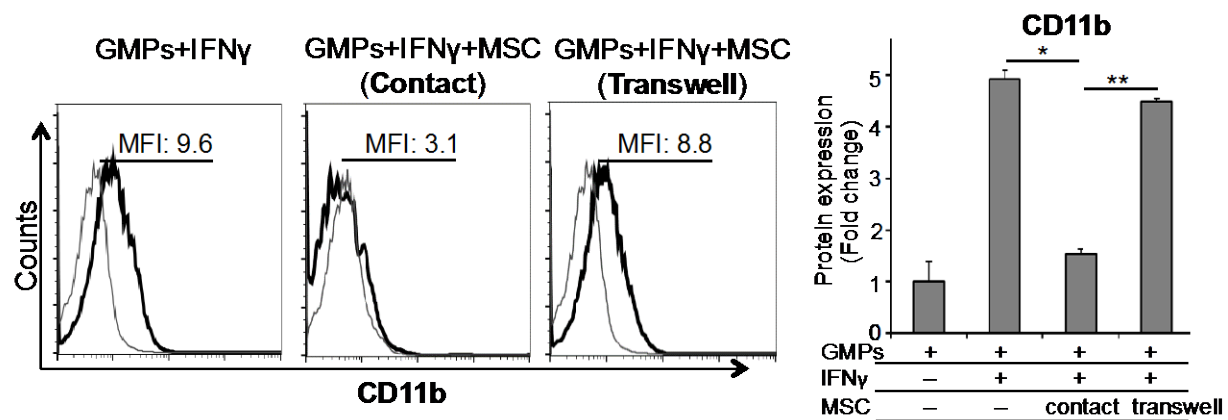

Figure 6. Effect of BM-MSC on GMP differentiation is contact dependent. BM-MSCs cultured indirectly with GMPs in the presence of Transwell fail to suppress CD11b surface marker acquisition and GMP differentiation into mature inflammatory cells.

Subaim 2.B. Define specific function of BM-MSC expressed factors promoting GMP differentiation into MDSC

(100% completion)   (January 2016- April 2016)

1) Major activities: To characterize the receptor involved in BM-MSC's contact-dependent immunoregulatory function

2) Specific objectives: To determine the mechanism by which in vitro expanded BM-MSC suppress GMP differentiation through cell-cell contact and the receptor involved in such contact dependency.

3) Significant results: Single cell suspension was prepared from in vitro expanded BM-MSC from C57BL/6 mice. In order to investigate the receptor involved in immunoregulatory function of BM-MSC, cells were screened for cell surface expressed inhibitory molecules including Programmed death-ligand 1 (PD-L1), V-set domain-containing T-cell activation inhibitor 1 (VTCN-1), CD200 and Carcinoembryonic antigen-related cell adhesion molecule 1 (CEACAM-1) receptors. mRNA expression levels of these candidate receptors was evaluated using real-time PCR. Our data demonstrated relatively higher expression levels of CD200 on BM-MSCs compared to other receptors **(Figure 7a)**. Furthermore, in order to assess the effect of IFNγ stimulation on upregulation of CD200, in vitro expanded BM-MSC

were stimulated with IFNγ for 18 hours and then using real-time PCR mRNA expression level of CD200 was investigated. These results further demonstrated that BM-MSCs significantly upregulate their expression of CD200 in the inflammatory environment **(Figure 7b)**. Many studies have suggested that the interaction between CD200 and its receptor (CD200R), which is expressed by myeloid cells, is involved in regulation of myeloid cell function. These observations and our PCR data demonstrating high mRNA expression of CD200 on MSCs, suggested to us that CD200 could be the critical receptor mediating the immunoregulatory effect of BM-MSC on GMPs. We then performed flow cytometry to confirm the expression of CD200 and its counter receptor, CD200R on BM-MSCs and GMPs, respectively. In vitro expanded BM-MSC and FACS sorted splenic GMPs were immunostained for CD200 and CD200R antibodies, respectively. As shown in **Figure 7c & d**, our FACS data confirmed the expression of CD200 and CD200R by MSCs and GMPs, respectively. Next, to investigate the role of CD200 expression by BM-MSC in mediating their suppressive effect on GMP differentiation, using CD200-shRNA, expression of CD200 was silenced on BM-MSCs. Then, either control-shRNA or CD200-shRNA BM-MSCs (5x10^5 cells) were co-cultured with GMP (1x10^6 cells) in the presence of pro-inflammatory cytokine IFNγ (100 ng/mL). After 72 hours, cultures were terminated and cells were immunostained for CD11b surface marker. As shown in **Figure 8**, while wild-type BM-MSCs (control-shRNA) suppressed GMP acquisition of CD11b differentiation marker, CD200-silenced BM-MSCs (CD200-shRNA) demonstrated significantly abrogated ability in suppressing GMP differentiation, further confirming the critical role of CD200 in the immunoregulatory function of BM-MSCs.
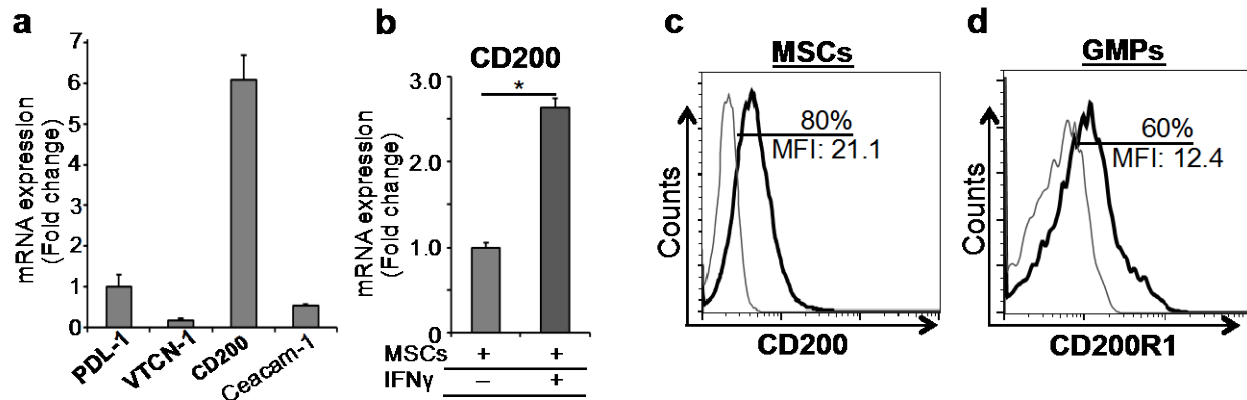

Figure 7. **(a)** Real-time PCR analysis of mRNA expression levels of PDL-1, VTCN-1, CD200 and Ceacam-1 by BM-MSCs. **(b)** Real-time PCR analysis of CD200 expression levels on resting versus IFNγ-stimulated BM-MSCs. **(c & d)** FACS plots demonstrating the expression of CD200 and CD200R1 by BM-MSCs and GMPs, respectively.
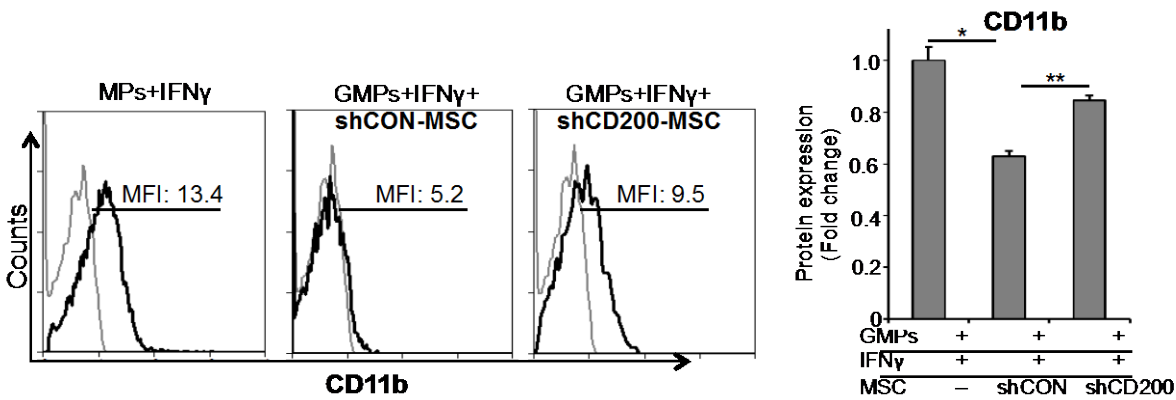
Figure 8. Regulatory effect of BM-MSCs on GMP differentiation depends on their expression of CD200. Unlike control-shRNA (wild-type) BM-MSCs, CD200-shRNA BM-MSCs fail to suppress acquisition of CD11b maturation marker by GMPs.

Task #3: Evaluate effect of in vivo administration of BM-MSC on MDSC frequency and ocular inflammation   (May 2016- December 2016)

Subaim 3.A. Assess effect of BM-MSC on frequencies of MDSC versus macrophages and on expression of inflammatory cytokines (IL-1β and TNF-α) in the eye
                                              (100% completion)   (May 2016- August 2016)

1) Major activities: To investigate the in vivo effect of BM-MSCs on ocular inflammation
2) Specific objectives: To investigate the in vivo effect of wild-type and CD200-silenced BM-MSC administration on frequencies of GMPs and mature inflammatory cells and expression of pro-inflammatory cytokines in corneal injury
3) Significant results: Corneal injury was induced in C57BL/6 mice by mechanical removal of the corneal epithelium and anterior stroma. Functional expression of CD200 was silenced in in vitro expanded MSCs using shRNA. Control shRNA (wild-type) or CD200 shRNA MSCs (0.5×10^6 cells per mouse) were intravenously injected through the tail vein to mice 1 hour after injury. Corneas were harvested 48 hour post-injury. Corneal single cell suspensions were made and immunostained with CD14, CD11b and CD45 mAbs to determine the frequencies of CD14$^+$CD11b$^-$ GMPs and CD45$^+$ inflammatory cells. Our flow cytometry results demonstrated an approximate 5-fold increase in the frequencies of corneal CD14$^+$ CD11b$^-$ GMPs in mice treated with control shRNA MSCs compared with non-treated mice (**Fig. 9a**). Interestingly, silencing of CD200 in MSCs abrogated their ability to expand corneal GMP frequencies (**Fig. 9a**). Next, we investigated the effect of administration of control shRNA versus CD200-shRNA treated MSCs on infiltration of inflammatory cells into the cornea after injury by assessing the frequencies of corneal CD45$^+$ cells. Flow cytometry data demonstrated that systemic administration of control shRNA MSCs resulted in significant suppression of inflammatory cell infiltration in the injured cornea. CD200-silenced MSCs were, however, unable to suppress the corneal infiltration of CD45$^+$ inflammatory cells (**Fig. 9b**). Next, real time PCR was performed for the expression of inflammatory cytokine IL-1β in the cornea. Similarly, PCR data demonstrated substantially lower transcript levels of IL-1β in conjunctiva of mice treated with control shRNA MSCs compared to untreated mice. Similar to flow cytometry results, CD200 silenced MSCs lost their ability

11

to suppress expression of inflammatory cytokine IL-1β in the injured cornea (**Fig. 9c**). Collectively, our data suggest that expression of CD200 by MSCs is essential for expansion of ocular GMPs and suppression of ocular inflammation.
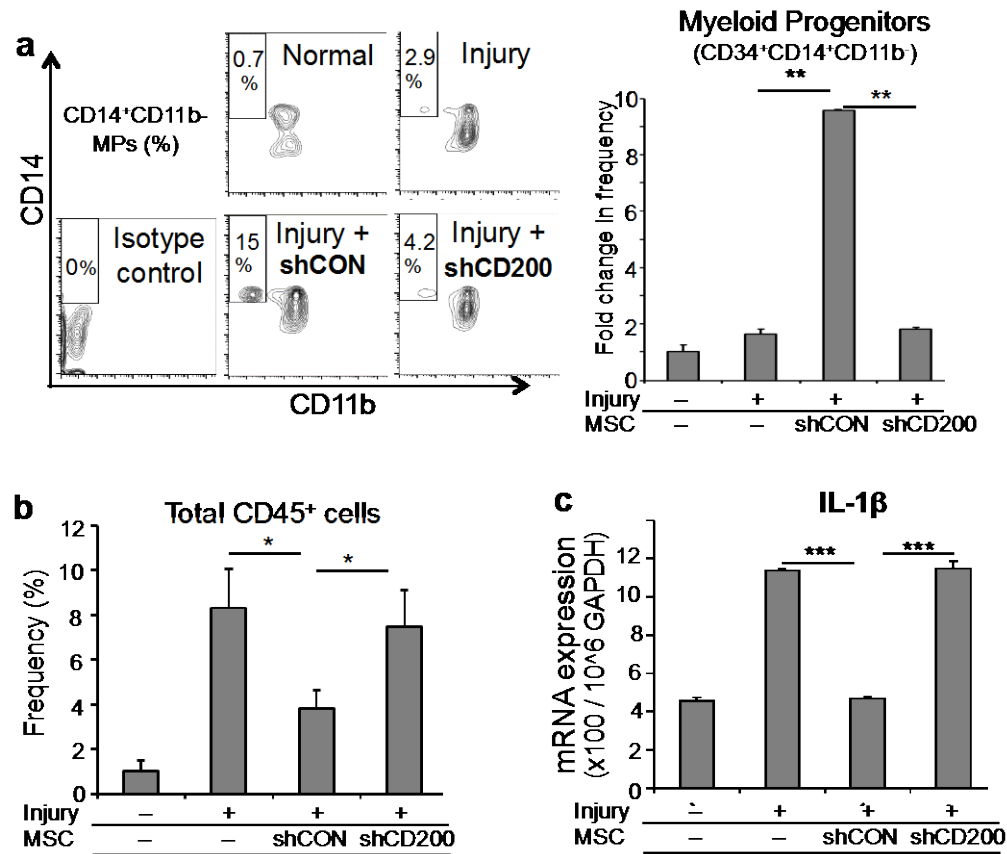

Figure 9. Systemic BM-MSC treatment suppresses ocular inflammation and expands corneal GMP frequencies. **(a)** Systemic treatment of mice with corneal injury with BM-MSC (shCON) leads to an approximate 5-fold increase in frequencies of corneal GMPs compared to mice treated with CD200-silenced MSCs (shCD200) or untreated mice. **(b)** Corneal injury leads to a significant increase in the frequencies of inflammatory CD45+ cells. Systemic treatment with BM-MSC (shCON) dramatically suppresses corneal CD45+ cell frequencies, while CD200-silenced BM-MSC (shCD200) show abrogated ability in suppressing CD45+ cell frequencies. **(c)** Systemic treatment with BM-MSC (shCON) results in a significant decrease in the transcript levels of inflammatory cytokine IL-1β in the eye compared to mice treated with CD200-silenced MSCs (shCD200) and untreated mice.

Subaim 3.B. Assess effect of BM-MSC on repair of corneal injury
                              (100% completion)   (September 2016- December 2016)

1) Major activities: To investigate the effect of BM-MSC treatment on corneal wound repair
2) Specific objectives: To determine the in vivo effect of wild-type and CD200 silenced MSCs on restoration of corneal structure after injury
3) Significant results: Corneal injury was induced in C57BL/6 mice by mechanical removal of the corneal epithelium and anterior stroma. Functional expression of CD200 was silenced in in vitro

expanded MSCs using shRNA. Control shRNA (wild-type) or CD200 shRNA MSCs (0.5×10^6 cells per mouse) were intravenously injected through the tail vein to mice 1 hour after injury. Corneas were harvested 48 hour post-injury. Corneal cross sections were prepared and fixed in 4% paraformaldehyde and stained with hematoxylin and eosin (H & E). Images were obtained using a bright field microscope at ×20 magnification. Our H& E staining results demonstrated significant cell infiltration, thinning of corneal epithelium and increased stromal thickness in injured corneas. However, systemic treatment with wild-type or control shRNA-treated MSCs resulted in less cell infiltration and significant restoration of normal corneal structure. Silencing of CD200 expression in MSCs abrogated their regenerative abilities and resulted in significant inflammatory cell infiltration and disruption of corneal structure **(Fig. 10)**.
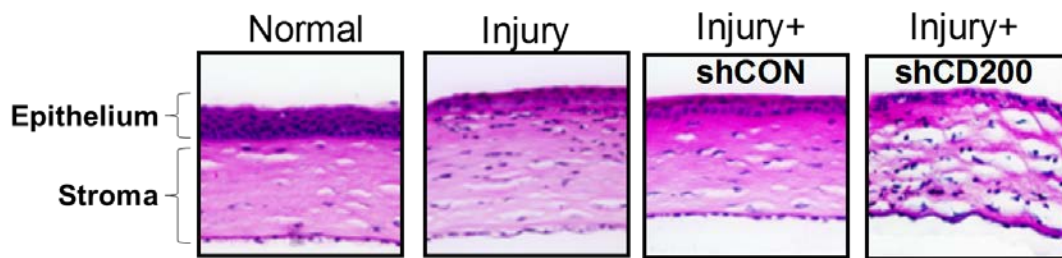

Figure 10. H &E staining of corneal cross-sections (×20) from normal, untreated, control-shRNA BM-MSC-treated and CD200-shRNA BM-MSC-treated mice demonstrating epithelial and stromal layers and inflammatory cell infiltration. Systemic treatment with wild-type BM-MSC (shCON) results in less cell infiltration and significant restoration of corneal structure. Silencing of CD200 expression in MSCs (shCD200) abrogates their ability to suppress immune cell infiltration and restore normal corneal structure.

Additional findings:
We also found that BM-MSCs secrete high levels of hepatocyte growth factor (HGF) in the inflammatory environment of the injured cornea. Our results demonstrated that BM-MSCs restore corneal transparency after injury by inhibiting the expression of opacity inducing α-SMA (α-smooth muscle actin) and TGF-β (transforming growth factor β) through secretion of HGF. In addition, we found that administration of HGF alone can suppress corneal opacity and inflammation.

●**What opportunities for training and professional development has the project provided?**

Abstract of the current findings was presented as a poster presentation in ARVO conference 2016 in Seattle, Washington. The poster was also selected as a finalist and was entered into the *members-in-training (MIT) outstanding poster award* competition and won the best poster award in the cornea study section.

●How were the results disseminated to communities of interest?

Abstract of the current findings was presented as a poster presentation in ARVO conference 2016 in Seattle, Washington.
Results of the current study have been submitted as an original research article to the *Stem Cells* journal and have been accepted for publication.

●What do you plan to do during the next reporting period to accomplish the goals?

Nothing to report.

4. IMPACT

●What was the impact on the development of the principal discipline(s) of the project?
Our novel findings have revealed the critical role of expression of CD200 by BM-MSC in mediating their regulatory function on the differentiation of myeloid progenitor cells. This observation has high translational value as it can serve as the background for the development of potential CD200-based therapies that could modulate the differentiation of progenitor cells to inflammatory cells at the very early stages of inflammation.

●What was the impact on other disciplines?
CD200-mediated suppression of tissue inflammation can also be investigated in other organ/tissue inflammatory diseases.

●What was the impact on technology transfer?
Nothing to report

●What was the impact on society beyond science and technology?
Findings from our study could significantly improve the public knowledge, as BM-MSCs have long been recognized for their substantial regenerative abilities and much less was known about the regulatory function of these cells on immune cells. Our results demonstrate that in addition to their regenerative capacity, BM-MSCs show immunoregulatory properties and have the ability to regulate the function of other immune cells during inflammation.

5. CHANGES/PROBLEMS

●Changes in approach and reasons for change
Nothing to report

●Actual or anticipated problems or delays and actions or plans to resolve them
Nothing to report

●**Changes that had a significant impact on expenditures**
Nothing to report

●**Significant changes in use or care of human subjects, vertebrate animals, biohazards, and/or select agents**
Nothing to report

6. PRODUCTS

●**Publications, conference papers, and presentations**

Abstract of the current findings was presented at the ARVO conference 2016 in Seattle, Washington.

- Amouzegar, A., Mittal, S., Chauhan, S.K. (2016). Mesenchymal stem cells modulate the differentiation of myeloid progenitor cells in corneal inflammation. Investigative Ophthalmology & Visual Science, 57 (12), 1434-1434. *(Winner of ARVO 2016 MIT Outstanding poster award)*

An original article on the major findings of the current project has been accepted for publication in the *Stem Cells* journal.

- Amouzegar, A., Mittal, S.K., Sahu, A., Sahu, S.K., Chauhan, S.K. (2017). Mesenchymal stem cells modulate differentiation of myeloid progenitor cells during inflammation. **Stem Cells**. (Accepted for publication)

An original article from the additional findings of this project has been published in the Stem Cell Reports.

- Mittal, S.K., Omoto, M., Amouzegar, A., Sahu, A., Rezazadeh, A., Katikireddy, K.R., Shah, D.I., Sahu, S.K. and Chauhan, S.K. (2016). Restoration of Corneal Transparency by Mesenchymal Stem Cells. **Stem Cell Reports**, 7(4), 583-590

●**Website(s) or other Internet site(s):** Nothing to report
●**Technologies or techniques:** Nothing to report
●**Inventions, patent applications, and/or licenses:** Nothing to report
●**Other products:** Nothing to report

7. PARTICIPANTS & OTHER COLLABORATING ORGANIZATIONS

●What individuals have worked on the project?

Name   : Sunil Chauhan, DVM, PhD
Project Role   : PI
Researcher Identifier   : eRA
Nearest person month worked : 2 months
Contribution to Project   : PI supervises all aspects of the project, including technical training of postdoctoral fellow, experimental design, troubleshooting, and data analysis. This also includes holding meetings with fellow (twice/week) to discuss progress and direction of the project.

Name   : Afsaneh Amouzegar, MD
Project Role   : Postdoctoral research Fellow
Researcher Identifier   : eRA ID: 12617641
Nearest person month worked: 24 months
Contribution to Project   : Under direct supervision of PI, research fellow is responsible for performing the experiments described in this project, collaborating on experimental design and analysis and presentation of data.

●Has there been a change in the active other support of the PD/PI(s) or senior/ley personnel since the last reporting period?
Nothing to report

●What other organizations were involved as partners?
Nothing to report

8. SPECIAL REPORTNG REQUIREMENTS
None

9. APPENDICES
        i). Quad Chart
        ii). Manuscripts – **a.** Stem Cells 2017, and **b.** Stem Cell Reports 2016

Modulation of Ocular Inflammation by Mesenchymal Stem Cells

MR130457 and Vision Research Program - Hypothesis Development Award
W81XWH-15-1-0024

PI: Sunil Chauhan, DVM, PhD   **Org:** Schepens Eye Research Institute   **Award Amount:** $249,828

Study/Product Aim(s)

1. Determine mesenchymal stem cell (BM-MSC)-mediated differentiation of immature myeloid progenitors (GMP) into myeloid-derived suppressor cells (MDSC).
2. Define critical factors expressed by BM-MSC that promote GMP differentiation into MDSC.
3. Evaluate effect of in vivo administration of BM-MSC on MDSC frequency and ocular inflammation.

Approach

We first plan to investigate BM-MSC-mediated differentiation of both bone marrow- and cornea-derived immature $CD14^+CD11b^{-/lo}$ progenitors into MDSC. Secondly, we will identify and functionally characterize the BM-MSC-expressed factors that promote MDSC generation. Finally, using a mouse model of corneal injury, we will determine the effect of systemic administration of in vitro expanded BM-MSC on MDSC frequency and ocular inflammation.
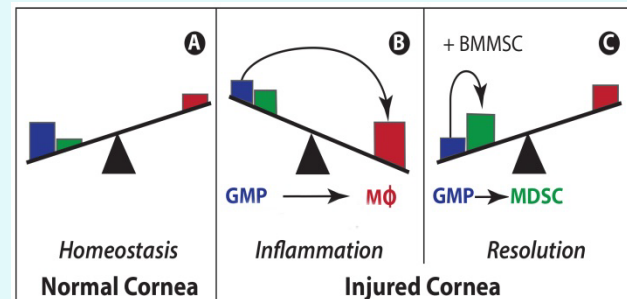

***Diagram depicting our hypothesis**. **A:** in normal cornea, immature myeloid progenitors (GMP), outnumber macrophages (MΦ); **B:** in corneal injury, GMP primarily differentiate into MΦ that promote inflammation; however, **C:** administration of BM-MSC promotes GMP differentiation into MDSC in the injured cornea and facilitates resolution of inflammation. The goal of this project is to delineate the as-of-yet-unknown mechanisms by which mesenchymal stem cells (BM-MSC) promote generation of immunoregulatory myeloid derived suppressor cells (MDSC) to control ocular inflammation.*

Accomplishment: - 1. Amouzegar, A., et al. MSCs modulate differentiation of myeloid progenitors during inflammation. Stem Cells, 2017 (In press)
2. Mittal, S.K. et al. Stem Cell Reports, 2016; 7(4), 583-590.

Timeline and Cost

Activities CY	14	15
1. BM-MSC-mediated differentiation of GMP into MDSC.	▮	
2. MDSC-promoting critical factors expressed by BM-MSC		▮
3. In vivo effects of BM-MSC on MDSC and ocular inflammation		▮
Text (Major aim/study/milestone)		
Estimated Budget ($)	**$127,321**	**$122,507**

Updated: (6th March 2017)

Goals/Milestones

☑ **IACUC/ACURO Approvals**

CY14 Goals –
Define mechanisms by which BM-MSC promote immature $CD14+CD11b^{-/lo}$ GMP differentiation into MDSC
☑ Culture bone marrow-derived GMP with MSC
☑ Co-culture corneal GMP with BM-MSC
☑ Evaluate BM-MSC expression of factors promoting MDSC

CY15 Goals –
☑ Assess function of BM-MSC factors promoting GMP into MDSC
☑ Effect of in vivo administered BM-MSC on MDSC frequency
☑ Effect of in vivo administered BM-MSC on ocular inflammation

Comments/Challenges/Issues/Concerns: None

Budget Expenditure to Date
Projected Expenditure: $ 249,828
Actual Expenditure: $ 249,828

ISSCR

Restoration of Corneal Transparency by Mesenchymal Stem Cells

Sharad K. Mittal,[1,2,6] Masahiro Omoto,[1,3,6] Afsaneh Amouzegar,[1,2] Anuradha Sahu,[1] Alexandra Rezazadeh,[1] Kishore R. Katikireddy,[1,2] Dhvanit I. Shah,[4] Srikant K. Sahu,[1,5] and Sunil K. Chauhan[1,2,*]

[1]Schepens Eye Research Institute, Massachusetts Eye and Ear, 20 Staniford Street, Boston, MA 02114, USA
[2]Department of Ophthalmology, Harvard Medical School, Boston, MA 02114, USA
[3]Department of Ophthalmology, Keio University School of Medicine, Tokyo 160-8582, Japan
[4]Brigham and Women's Hospital, Harvard Medical School, Boston, MA 02114, USA
[5]L.V. Prasad Eye Institute, Bhubaneswar, Odisha 751024, India
[6]Co-first author
*Correspondence: sunil_chauhan@meei.harvard.edu
http://dx.doi.org/10.1016/j.stemcr.2016.09.001

SUMMARY

Transparency of the cornea is indispensable for optimal vision. Ocular trauma is a leading cause of corneal opacity, leading to 25 million cases of blindness annually. Recently, mesenchymal stem cells (MSCs) have gained prominence due to their inflammation-suppressing and tissue repair functions. Here, we investigate the potential of MSCs to restore corneal transparency following ocular injury. Using an in vivo mouse model of ocular injury, we report that MSCs have the capacity to restore corneal transparency by secreting high levels of hepatocyte growth factor (HGF). Interestingly, our data also show that HGF alone can restore corneal transparency, an observation that has translational implications for the development of HGF-based therapy.

INTRODUCTION

A transparent cornea is crucial for optimal vision. Ocular trauma, a leading cause of loss of corneal transparency, accounts for approximately 25 million cases of blindness annually (Resnikoff et al., 2008; Whitcher et al., 2001). During ocular injury, inflammation-induced transforming growth factor β (TGF-β), particularly TGF-β1 and TGF-β2, drive the differentiation of corneal fibroblasts (activated keratocytes) into α-smooth muscle actin (αSMA)-expressing myofibroblasts (Jester et al., 1997; Torricelli et al., 2016), which are themselves opaque and produce disorganized extracellular matrix, leading to the development of corneal opacity and scarring (Jester, 2008; Jester et al., 2012; Ljubimov and Saghizadeh, 2015). Recently, mesenchymal stem cells (MSCs) have been linked to a variety of anti-inflammatory and repair functions in both ocular and non-ocular tissue injuries (Basu et al., 2014; Jiang et al., 2002; Lan et al., 2012; Lee et al., 2014; Uccelli et al., 2008; Wang et al., 2011). However, ocular injuries involving the cornea undergo a wound-healing process that often results in scar formation and loss of corneal transparency. Here, we report that bone marrow-derived MSCs are capable of restoring corneal transparency after injury involving corneal stroma. Specifically, we show that MSCs secrete high levels of hepatocyte growth factor (HGF), which inhibits the generation of opacity-inducing myofibroblasts. Furthermore, we show that HGF alone can restore corneal transparency in an in vivo model of eye injury, a finding that offers an HGF-based therapeutic approach that could potentially eliminate the need for cell-based and conventional therapies.

RESULTS AND DISCUSSION

Inflammatory Milieu Drives MSCs to Secrete Elevated Levels of HGF

The cornea is the most anterior tissue of the eye that comprises the epithelium, stroma, and endothelium (Nishida and Saika, 2011). Ocular injuries involving the stroma (Figure 1A) lead to corneal scarring and compromised vision (Jester, 2008; Whitcher et al., 2001). The aim of this study was to determine whether MSCs have the potential to restore corneal transparency following injury. To investigate this, we first screened MSCs for expression of potential anti-inflammatory and growth factors under both homeostasis and inflammatory conditions. In vitro expanded and functionally characterized bone marrow-derived MSCs (Figures 1B and 1C) were cultured in the absence (medium alone) or presence of interleukin-1β (IL-1β) (to mimic injury-induced inflammatory milieu) for 24 hr, followed by quantification of tumor necrosis factor-stimulated gene 6 (Tsg-6), Il-10, Tgf-β1, and Hgf transcripts using real-time qPCR (Figure 1D). Strikingly, IL-1β stimulation greatly enhanced the expression of Hgf in MSCs compared with unstimulated cells. In contrast, Tgf-β1 expression was significantly reduced in IL-1β-stimulated MSCs. The steady-state expression of Tsg-6 was moderately increased, and Il-10 remained unchanged upon IL-1β stimulation. In addition, ELISA performed on culture supernatants corroborated the qPCR data and showed a 2.5-fold increase in HGF secretion by IL1β-stimulated MSCs (Figure 1E). These in vitro data demonstrate that MSCs express high levels of HGF in an inflamed environment. We also confirmed these findings using human MSCs. Our data showed that human
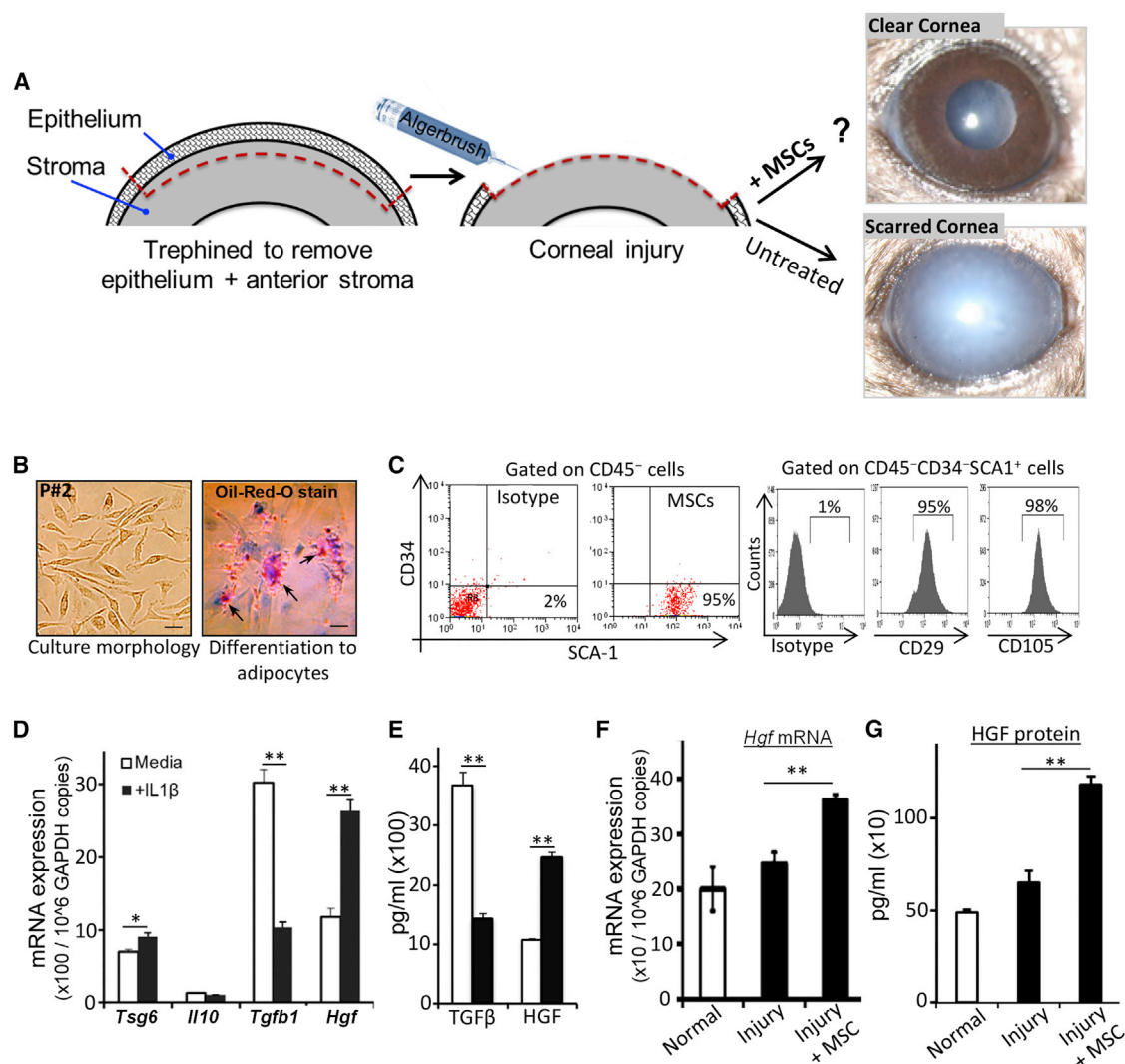
Figure 1. MSCs Secrete High Levels of HGF upon Stimulation with IL-1β

(A) Schematic showing injury model of mouse cornea created by mechanical removal of epithelium and anterior stroma, and effect of mesenchymal stem cell (MSC) administration on corneal opacity.

(B) Micrographs showing MSC morphology in culture at second passage, and differentiation of MSCs into adipocytes. MSCs were cultured in adipogenic medium for 2 weeks and stained with oil red O dye; red-colored vacuoles (arrows) were observed within the cytoplasm, indicating their differentiation into adipocytes. Scale bar, 25 μm.

(C) Phenotypic characterization of in vitro expanded MSCs using flow cytometry confirmed their surface phenotype of CD45−CD34−SCA1+CD29+CD105+ cells.

(D) MSCs were cultured in medium alone or with IL-1β for 24 hr. mRNA expression of indicated genes in MSCs were analyzed using real-time PCR.

(E) Protein expression of TGF-β1 and HGF was confirmed in culture supernatants of MSCs cultured in the presence or absence of IL-1β for 24 hr using ELISA. The values of mRNA and protein expression are shown as mean ± SD of three independent experiments.

(F and G) In vitro expanded MSCs were intravenously injected into the C57BL/6 mice 1 hr after corneal injury. Healthy corneas without injury were used as normal control. Corneas were harvested after 3 days, and (F) mRNA and (G) protein expressions of HGF were measured using real-time PCR and ELISA, respectively.

The values shown are mean ± SD and each corneal injury group consists of n = 6 mice. *p < 0.003, **p < 0.0001.

bone marrow-derived MSCs constitutively expressed high levels of HGF, which was significantly upregulated upon stimulation with recombinant human IL-1β (Figure S1A).

To determine whether in vivo administration of MSCs leads to high levels of HGF at inflamed injury site, we utilized a well-characterized sterile injury model of mouse
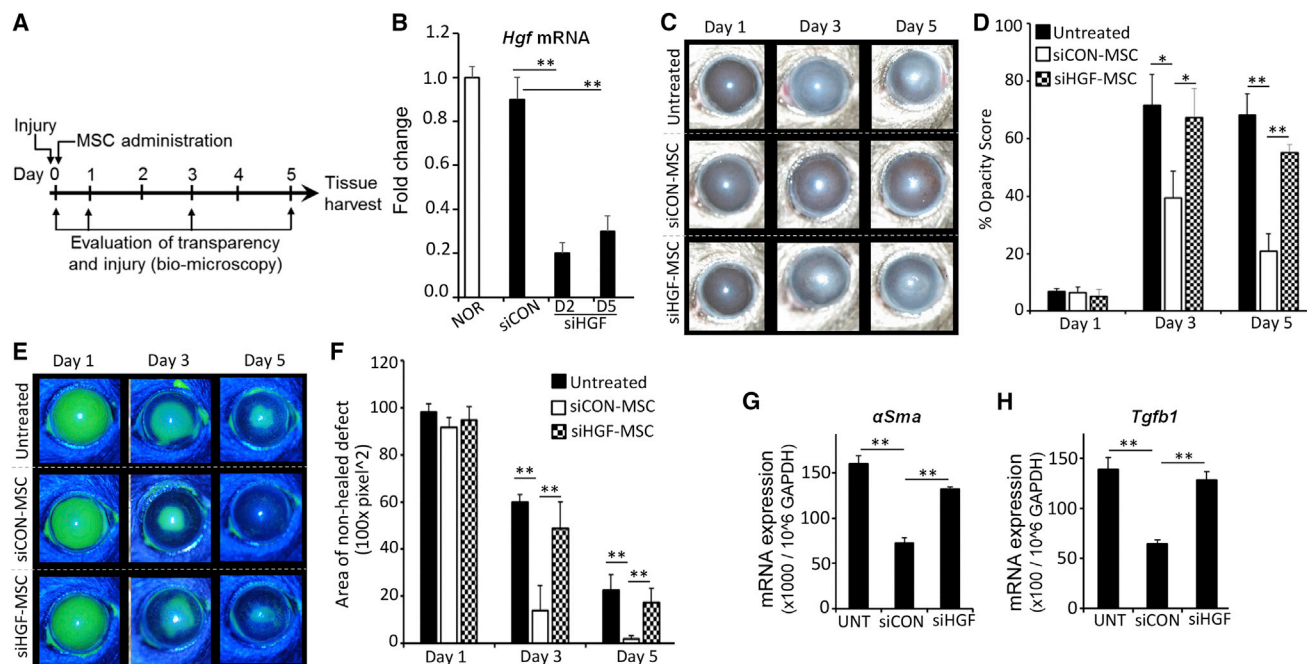
Figure 2. Restoration of Corneal Transparency Is Dependent upon HGF Expression by MSCs

(A) Schematic of experimental design.

(B) Real-time PCR analysis showing efficacy of *Hgf*-specific siRNA (siHGF) versus control siRNA (siCON) on downregulation of HGF expression in mesenchymal stem cells (MSCs). After corneal injury was induced in C57BL/6 mice, MSCs treated with control or *Hgf*-specific siRNA were intravenously administered 1 hr post injury and followed for 5 days. At days 1, 3, and 5 post injury, photographs of injured cornea with or without green fluorescein stain were captured using slit-lamp biomicroscopy. Corneal fluorescein staining was used to indicate epithelial defects and bright-field micrographs were used to evaluate corneal opacity.

(C and D) Representative bright-field microscopic images of injured cornea (C) were quantitated using Image J software to measure the corneal opacity scores (D).

(E) Representative biomicroscopic images showing green fluorescein-stained injured cornea.

(F) The fluorescein-stained area was quantitated using ImageJ software. A smaller area of fluorescein staining represents faster repair of corneal injury.

(G and H) At day 5 post injury, corneas were harvested. Total RNA was isolated from harvested corneas, and real-time PCR was performed to analyze mRNA expression of (G) α-*Sma* and (H) *Tgf-β1*.

The values shown are mean ± SD and each corneal injury group consists of n = 6 mice. *p < 0.02, **p < 0.005.

cornea (Basu et al., 2014; Hutcheon et al., 2007). Injury was induced by mechanical removal of corneal epithelium and anterior stroma (Figure 1A); 1 hr after injury, MSCs ($5 \times 10^5/0.1$ mL/mouse) were intravenously injected in mice. Using GFP-expressing MSCs (Figure S2), we additionally confirmed that MSCs specifically home to the injured eye (Lan et al., 2012; Omoto et al., 2014). Normal corneas without injury and corneas with injury alone (without MSC administration) served as controls. On day 3 after injury, corneas were harvested, and qPCR and ELISA were performed to measure HGF levels. Indeed, injured corneas from MSC-injected mice showed significantly higher levels of HGF at both transcript (Figure 1F) and protein (Figure 1G) levels compared with injured and normal corneas.

Capacity of MSCs to Restore Corneal Transparency Is Dependent upon Their HGF Expression

Based on our in vivo data and because previous reports have ascribed an anti-fibrotic function for HGF (Herrero-Fresneda et al., 2006), we hypothesized that HGF could be a putative MSC-expressed factor that could contribute to the restoration of transparency in injured corneas. We therefore determined whether altering HGF expression within MSCs influenced opacity in a sterile injury model of mouse cornea (Figures 1A and 2A). HGF expression in MSCs was knocked down using small interfering RNA (siRNA) (Abed et al., 2015), which led to nearly 80% reduction of *Hgf* expression compared with control siRNA (Figure 2B). MSCs transfected with *Hgf* siRNA or control siRNA were pre-stimulated with IL-1β for 6 hr, then intravenously

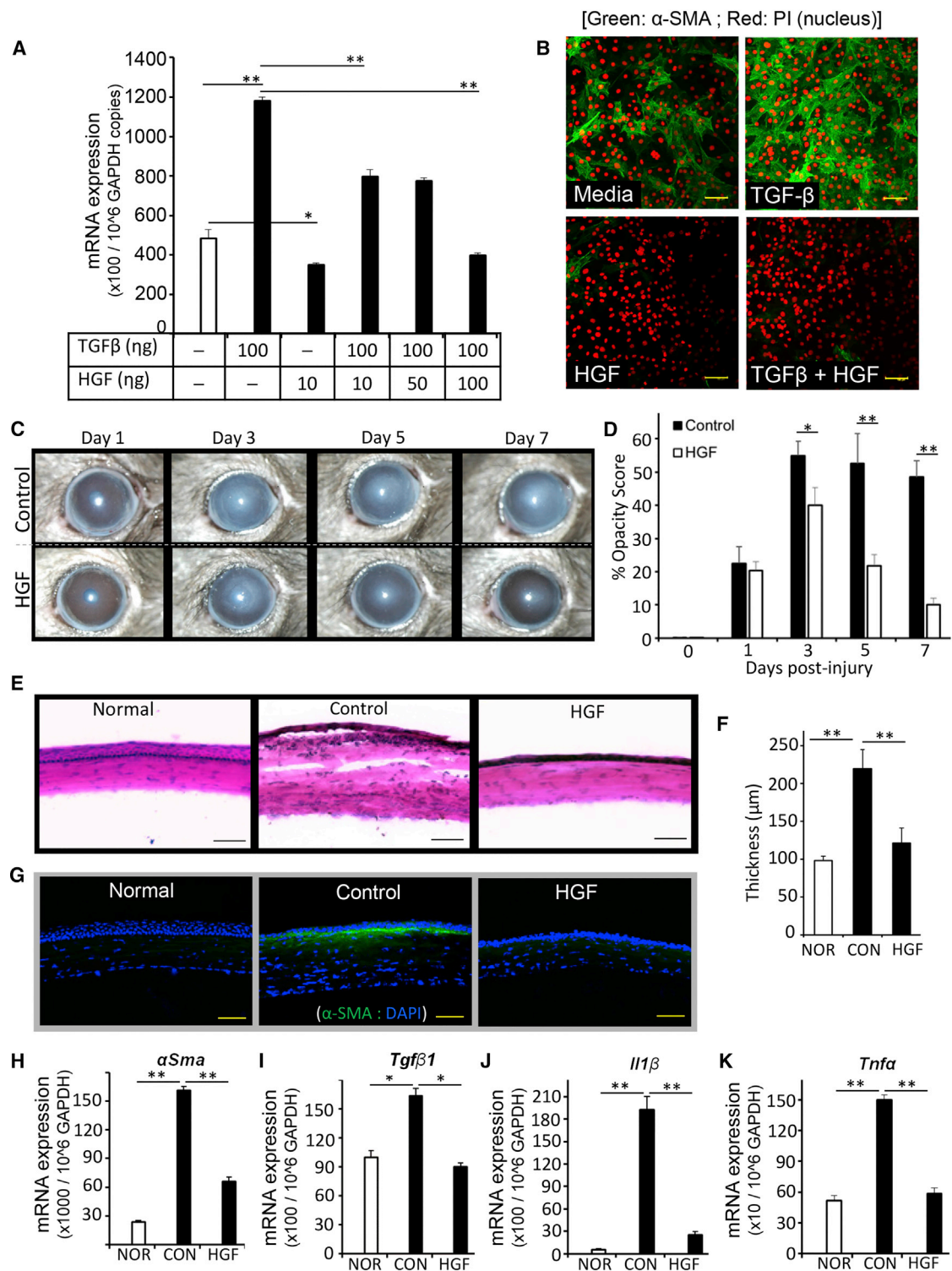**Figure 3. HGF Alone Is Sufficient to Inhibit Corneal Opacity and Inflammation**

(A and B) A corneal fibroblast cell line (MK/T1) was stimulated with TGF-β1 in the presence or absence of HGF for 24 hr. α-SMA expression was assessed (A) at mRNA level using real-time PCR and (B) at protein level by immunohistochemistry. The values shown are the mean ± SD of three independent experiments.

(legend continued on next page)

administered to the mice 1 hr post injury. Injured corneas with no MSC administration served as untreated controls. Slit-lamp biomicroscopy was used to monitor the extent of corneal opacity and wound healing for 5 days. Corneas of mice injected with control siRNA-treated MSCs showed a significant reduction in corneal opacity at days 3 and 5 post injury compared with corneas from *Hgf* siRNA-treated MSCs and untreated mice (Figures 2C and 2D). To determine the extent of wound repair, we used corneal fluorescein staining to assess the epithelial defect (Figures 2E and 2F). A smaller area of fluorescein (green) represents a faster rate of wound healing. A complete and significantly more rapid wound repair was seen in mice injected with control siRNA-treated MSCs compared with corneas from *Hgf* siRNA-treated MSCs and untreated control mice. Previous reports have shown similar effects of wild-type MSCs on wound repair (Lan et al., 2012; Lee et al., 2014). After 5 days of injury, corneas were harvested to assess expression levels of *α-Sma* and *Tgf-β1* using qPCR. Data showed a markedly decreased expression of *α-Sma* and its inducer cytokine *Tgf-β* (Yi et al., 2014) in the corneas of mice injected with control siRNA-treated MSCs compared with the corneas of *Hgf* siRNA-treated MSCs and untreated mice (Figures 2G and 2H). These data clearly demonstrate that HGF expression by MSCs is crucial for inhibiting the expression of opacity-inducing α-SMA and TGF-β, and restoring corneal transparency in the injured eye.

Topical Administration of HGF Alone Is Sufficient to Restore Corneal Transparency in Ocular Injury

Finally, the functional and translational relevance of HGF in restoring corneal transparency was confirmed by investigating the effect of HGF alone (without MSC administration) using both in vitro and in vivo model systems. First, to experimentally address whether HGF can inhibit expression of α-SMA in corneal fibroblasts, we stimulated a well-characterized corneal fibroblast cell line (MK/T1) (Gendron et al., 2001) with TGF-β1 in the absence or presence of recombinant mouse HGF for 24 hr. Unstimulated cultures served as a control. HGF treatment showed a dose-dependent suppression of TGF-β-induced *α-Sma* expression in corneal fibroblasts (Figure 3A). Consistent with our data in mice, we also observed that human recombinant HGF completely suppressed TGF-β1-induced *α-SMA* expression in human corneal fibroblasts (Figure S1B).

We also confirmed the effect of HGF on TGF-β-induced α-SMA protein expression using immunohistochemistry. HGF completely suppressed TGF-β-stimulated α-SMA protein expression in corneal fibroblasts and prevented their conversion to myofibroblasts (α-SMA⁺ cells: green) (Figure 3B), which are the primary cause of corneal opacity (Jester, 2008; Jiang et al., 2002). Interestingly, HGF treatment (Figures 3A and 3B; media versus HGF) also significantly reduced the baseline expression of α-SMA in corneal fibroblasts, suggesting that HGF alone could be effective in reversing pre-formed myofibroblasts into α-SMA-negative fibroblasts. Using this information, we sought to investigate whether in vivo administration of HGF can suppress corneal opacity. Corneal injury was induced as described above (Figure 1A), 5 μL of 0.1% recombinant mouse HGF or mouse serum albumin (control) was applied topically to the injured eye twice daily for up to 7 days after injury, and slit-lamp biomicroscopy was used to monitor corneal opacity (Figure 3C). At day 3 post injury, both groups showed a significant development of corneal opacity. However, the corneas of HGF-treated mice exhibited a significant reduction in opacity on day 5 and a near complete restoration of transparency on day 7 compared with mouse albumin-treated control corneas (Figure 3D). After 7 days post injury, corneas were harvested to confirm the effect of HGF on injury-induced opacity at cellular and molecular levels. H&E staining of corneal cross-sections revealed normalization of corneal tissue structures only in HGF-treated mice (Figure 3E), whereas albumin-treated control corneas showed a significant increase in tissue thickness accompanied by infiltration of inflammatory cells (Figures 3E and 3F). Moreover, HGF-treated corneas showed increased stratification of the epithelial cell layer (Figures S3A and S3B). Both confocal micrographs of immunostained corneas (Figure 3G) and qPCR (Figure 3H) showed a significant reduction in the expression of α-SMA in HGF-treated corneas compared with control corneas. Moreover, mRNA expression levels of α-SMA-inducer cytokine *Tgf-β1* (Figure 3I), and the inflammatory cytokines *Il-1β* (Figure 3J) and *Tnf-α* (Figure 3K) were significantly reduced in HGF-treated corneas compared with

(C–K) Corneal injury was induced by mechanical removal of corneal epithelium and anterior stroma in C57BL/6 mice. Thereafter, 5 μL of 0.1% murine recombinant HGF in PBS per eye was applied topically to the injured eye twice a day up to 7 days after injury. A control group received a similar dosage of mouse serum albumin. At days 1, 3, 5, and 7 post injury, bright-field photographs of injured corneas were captured to evaluate corneal opacity using slit-lamp biomicroscopy. Representative bright-field images of injured corneas (C) were quantitated using Image J software to assess corneal opacity scores (D). Corneas were harvested at 7 days post injury. Cross-sections were stained with H&E to visualize corneal tissue structure and infiltration of inflammatory cells (E), and measure corneal tissue thickness (F). For immunocytochemistry analysis (G), cross-sections were immunostained with the fibrosis marker α-SMA (green). In addition, harvested corneas were analyzed for their mRNA expression of (H) *α-Sma*, (I) *Tgf-β1*, (J) *Il-1β*, and (K) *Tnf-α* using real-time PCR.
The values shown are mean ± SD and each corneal injury group consists of n = 6 mice. *p < 0.01, **p < 0.005. Scale bars, 50 μm.

albumin-treated corneas. The fact that HGF-treated corneas showed high expression of *Hgf-R* (*c-Met*) compared with control corneas (Figure S3C) further supports our finding that HGF signaling inhibits α-SMA expression. Collectively, these findings indicate that HGF administration alone is sufficient to restore transparency in corneal injury by suppressing conversion of corneal fibroblasts into αSMA+ myofibroblasts and by inhibiting tissue infiltration of inflammatory cells, which secrete inflammatory cytokines and proteolytic enzymes, leading to degradation and remodeling of the extracellular matrix (Ljubimov and Saghizadeh, 2015).

Conventional treatments for ocular injuries involving corneal scarring vary from topical immunosuppressive steroids to corneal transplantation. However, (1) the increased risk of infection and delayed wound healing, (2) immune rejection of the transplant, and (3) shortage of cornea donors remain major limitations to such treatment (Hamil, 2011). Recently, due to their unique immunomodulatory property, MSCs have been used in experimental and clinical settings to treat a variety of tissue injuries and inflammatory diseases (Basu et al., 2014; Lan et al., 2012; Lee et al., 2014; Uccelli et al., 2008; Wang et al., 2011). Here, we ascribe a hitherto unknown function of MSCs in restoring corneal transparency following ocular injury. We report that MSCs inhibit the expression of opacity-inducing α-SMA and its inducer TGF-β in the injured cornea by secreting HGF. Furthermore, we show that administration of HGF alone can suppress corneal opacity and inflammation. Given that clinical-grade production of cell-based therapies is cost prohibitive, our findings offer the promise of HGF-based modalities for treating ocular conditions that compromise corneal transparency and vision.

EXPERIMENTAL PROCEDURES

Animals
Six- to 8-week-old male C57BL/6 wild-type mice (Charles River Laboratories) were used in these experiments. The protocol was approved by the Schepens Eye Research Institute Animal Care and Use Committee, and all animals were treated according to the ARVO Statement for the Use of Animals in Ophthalmic and Vision Research.

Corneal Injury
Mice were anesthetized and a 3-mm superficial keratectomy was performed as previously described (Basu et al., 2014; Hutcheon et al., 2007). In brief, under a dissecting microscope the central area of the cornea was demarcated with a 3-mm trephine and rotated gently to cut into the stroma. The circular area was traced with a sharp pair of surgical forceps, and the corneal epithelium and basement membrane, including the anterior portion of the

stroma, were removed using a hand-held Algerbrush II (Alger Equipment). Following injury, corneas were flushed with sterile saline and subsequently covered with Vetropolycin (bacitracin-neomycin-polymyxin) ophthalmic ointment.

Corneal opacity was determined by taking bright-field images using a biomicroscope. Corneal wounds were monitored by placing 1 μL of 2.5% sodium fluorescein (vital staining) on the ocular surface. After 3 min, the ocular surface was visualized by slit-lamp biomicroscope under cobalt blue light, and digital pictures of corneal defects were captured. Degree of opacity and area of injury (fluorescein-stained green color) were calculated using the NIH ImageJ (version 1.34s) software.

Isolation, Expansion, and Characterization of MSCs
Bone marrow was harvested from femurs of euthanized C57BL/6 mice. MSCs were phenotypically and functionally characterized as per criteria defined by The International Society for Cellular Therapy (Dominici et al., 2006), using the previously described plastic adherence method of MSC cultivation (Lan et al., 2012; Lee et al., 2014), and bone marrow cells were cultured in murine MSC-specific MesenCult medium with supplement (STEMCELL Technologies). Non-adherent cells were removed by changing medium every 2 days, and at passage 2 the MSCs were harvested to be used in experiments. Before using MSCs in indicated experiments, cells were characterized phenotypically for the expression of MSC markers (CD45−CD34−SCA1+CD29+CD105+) by flow cytometry and functionally by their in vitro differentiation into adipocytes using MesenCult adipogenic stimulatory supplements (STEMCELL). Oil red O (Sigma-Aldrich) staining was used to confirm the differentiation of MSCs into the adipocytes.

siRNA Transfection
MSCs (1.5×10^6 cells) were plated in a 75-cm² flask and incubated for 18–24 hr to reach to 60%–70% confluency. The cells were then washed and transfected with 4.8 μg of *Hgf*-specific or non-specific control siRNA duplex using transfection reagent in siRNA transfection medium according to the protocol suggested by the manufacturer (Santa Cruz Biotechnology). After overnight incubation, transfection medium was replaced with normal MSC growth culture medium and cells were cultured for an additional 2 days. Knockdown efficiency of siRNA was validated by real-time PCR using *Hgf*-specific primers after 2 and 5 days of transfection.

MSC or HGF Administration
In vitro expanded wild-type or *Hgf*-silenced MSCs were pre-stimulated with IL-1β for 6 hr, and 5×10^5 MSCs in 100 μL of normal saline per mouse were injected to mice 1 hr after corneal injury. Mice were placed in a restraining tube without anesthesia and the tail cleaned with 70% ethanol. The tail was pulled gently and cells in 100 μL of PBS were injected into the tail vein. Five microliters of 0.1% murine recombinant HGF protein (R&D Systems) or mouse serum albumin (Sigma-Aldrich) was applied topically to the injured eye twice daily for up to 7 days after injury.

In Vitro MK/T1 Cell Stimulation
The mouse corneal fibroblast cell line MK/T1 (Gendron et al., 2001) was seeded at 1×10^5 cells per well in 24-well plates and

cultured in medium alone or stimulated with 100 ng/mL murine recombinant TGF-β1 (R&D Systems) in the presence or absence of murine recombinant HGF (R&D Systems) at indicated doses for 24 hr. Cells were then used for evaluation of *α-Sma* expression by real-time PCR and immunohistochemistry.

RNA Isolation and Real-Time qPCR

Total RNA was isolated using the RNeasy Micro Kit (Qiagen). Isolated RNA was reverse transcribed into cDNA using oligo(dT) primer and SuperScript III (Invitrogen). Real-time qPCR was then performed using Taqman Universal PCR Mastermix and pre-formulated Taqman primers for murine glyceraldehyde-3-phosphate dehydrogenase (*Gapdh*), *Hgf*, *Il-10*, *Tsg6*, *Il-1β*, *Tgf-β1*, *Tnf-α*, and *α-Sma* (Life Technologies). The results were analyzed by the comparative threshold cycle method and normalized to *Gapdh* as an internal control.

Immunohistochemistry and Histology

Cryosections of the whole eyeball and fibroblast culture on 8-chamber slides were fixed in acetone and blocked with 2% BSA and anti-FcR antibodies (catalog #14-0161-86, Affymetrix eBioscience). The sections were immunostained with Alexa Fluor 488-conjugated anti-α-SMA or isotype-matched control antibodies (#53-6496-80, Affymetrix) overnight at 4°C. Slides were then mounted using Vector Shield mounting medium (Vector Laboratories) and examined under a confocal microscope. For histological evaluation, corneal sections were stained with H&E and examined using bright-field microscopy.

Flow Cytometry

A single-cell suspension of MSCs was prepared and stained with fluorochrome-conjugated monoclonal antibodies and appropriate isotype controls. Antibodies (Biolegend) against CD45 (catalog #103133), CD34 (#119310), SCA-1 (#108105), CD29 (#102207), and CD105 (#120407) were used for the phenotypic characterization of MSCs. Stained cells were analyzed on an LSR-II flow cytometer (BD Biosciences).

ELISA

Levels of TGF-β1 and HGF in supernatants of MSC cultures or corneal lysates were analyzed using commercially available murine ELISA kits (R&D Systems) as per the manufacturer's instructions.

Statistical Analysis

Mann-Whitney U tests or Student's t tests were performed to determine significance, which was set at p < 0.05. Results are presented as the mean ± SD of three independent experiments. In vivo evaluations and quantification of images of corneal injury and opacity were performed in a masked fashion. Samples sizes were estimated on the basis of previous experimental studies on corneal injury and inflammation (Lan et al., 2012; Basu et al., 2014).

SUPPLEMENTAL INFORMATION

Supplemental Information includes three figures and can be found with this article online at http://dx.doi.org/10.1016/j.stemcr.2016.09.001.

AUTHOR CONTRIBUTIONS

S.K.M. and M.O. performed experiments, and contributed to data analysis and manuscript writing. A.A., A.S., A.R., and K.R.K. assisted in performing experiments and data analysis. S.K.S. contributed to manuscript revision and data analysis. D.I.S. assisted in GFP-MSC homing experiments. S.K.C. contributed to the underlying hypothesis, designed the experiments, analyzed data, and wrote the manuscript.

REFERENCES

Abed, E., Bouvard, B., Martineau, X., Jouzeau, J.-Y., Reboul, P., and Lajeunesse, D. (2015). Elevated hepatocyte growth factor levels in osteoarthritis osteoblasts contribute to their altered response to bone morphogenetic protein-2 and reduced mineralization capacity. Bone 75, 111–119.

Basu, S., Hertsenberg, A.J., Funderburgh, M.L., Burrow, M.K., Mann, M.M., Du, Y., Lathrop, K.L., Syed-Picard, F.N., Adams, S.M., Birk, D.E., et al. (2014). Human limbal biopsy-derived stromal stem cells prevent corneal scarring. Sci. Transl. Med. 6, 266ra172.

Dominici, M., Le Blanc, K., Mueller, I., Slaper-Cortenbach, I., Marini, F., Krause, D., Deans, R., Keating, A., Prockop, D., and Horwitz, E. (2006). Minimal criteria for defining multipotent mesenchymal stromal cells. The International Society for Cellular Therapy position statement. Cytotherapy 8, 315–317.

Gendron, R.L., Liu, C.Y., Paradis, H., Adams, L.C., and Kao, W.W. (2001). MK/T-1, an immortalized fibroblast cell line derived using cultures of mouse corneal stroma. Mol. Vis. 7, 107–113.

Hamil, M.B. (2011). Mechanical injury. In Cornea, J.H. Krachmer, M. Mannis, and E.J. Holland, eds. (Mosby | Elsevier), pp. 1169–1185.

Herrero-Fresneda, I., Torras, J., Franquesa, M., Vidal, A., Cruzado, J.M., Lloberas, N., Fillat, C., and Grinyó, J.M. (2006). HGF gene therapy attenuates renal allograft scarring by preventing the profibrotic inflammatory-induced mechanisms. Kidney Int. 70, 265–274.

Hutcheon, A.E.K., Sippel, K.C., and Zieske, J.D. (2007). Examination of the restoration of epithelial barrier function following superficial keratectomy. Exp. Eye Res. *84*, 32–38.

Jester, J.V. (2008). Corneal crystallins and the development of cellular transparency. Semin. Cell Dev. Biol. *19*, 82–93.

Jester, J.V., Barry-Lane, P.A., Petroll, W.M., Olsen, D.R., and Cavanagh, H.D. (1997). Inhibition of corneal fibrosis by topical application of blocking antibodies to TGF beta in the rabbit. Cornea *16*, 177–187.

Jester, J.V., Brown, D., Pappa, A., and Vasiliou, V. (2012). Myofibroblast differentiation modulates keratocyte crystallin protein expression, concentration, and cellular light scattering. Invest. Ophthalmol. Vis. Sci. *53*, 770–778.

Jiang, Y., Jahagirdar, B.N., Reinhardt, R.L., Schwartz, R.E., Keene, C.D., Ortiz-Gonzalez, X.R., Reyes, M., Lenvik, T., Lund, T., Blackstad, M., et al. (2002). Pluripotency of mesenchymal stem cells derived from adult marrow. Nature *418*, 41–49.

Lan, Y., Kodati, S., Lee, H.S., Omoto, M., Jin, Y., and Chauhan, S.K. (2012). Kinetics and function of mesenchymal stem cells in corneal injury. Invest. Ophthalmol. Vis. Sci. *53*, 3638–3644.

Lee, R.H., Yu, J.M., Foskett, A.M., Peltier, G., Reneau, J.C., Bazhanov, N., Oh, J.Y., and Prockop, D.J. (2014). TSG-6 as a biomarker to predict efficacy of human mesenchymal stem/progenitor cells (hMSCs) in modulating sterile inflammation in vivo. Proc. Natl. Acad. Sci. USA *111*, 16766–16771.

Ljubimov, A.V., and Saghizadeh, M. (2015). Progress in corneal wound healing. Prog. Retin. Eye Res. *49*, 17–45.

Nishida, T., and Saika, S. (2011). Cornea and sclera. In Cornea, J.H. Krachmer, M. Mannis, and E.J. Holland, eds. (Mosby | Elsevier), pp. 3–24.

Omoto, M., Katikireddy, K.R., Rezazadeh, A., Dohlman, T.H., and Chauhan, S.K. (2014). Mesenchymal stem cells home to inflamed ocular surface and suppress allosensitization in corneal transplantation. Invest. Ophthalmol. Vis. Sci. *55*, 6631–6638.

Resnikoff, S., Pascolini, D., Mariotti, S.P., and Pokharel, G.P. (2008). Global magnitude of visual impairment caused by uncorrected refractive errors in 2004. Bull. World Health Organ. *86*, 63–70.

Torricelli, A.A.M., Santhanam, A., Wu, J., Singh, V., and Wilson, S.E. (2016). The corneal fibrosis response to epithelial-stromal injury. Exp. Eye Res. *142*, 110–118.

Uccelli, A., Moretta, L., and Pistoia, V. (2008). Mesenchymal stem cells in health and disease. Nat. Rev. Immunol. *8*, 726–736.

Wang, J., Liao, L., and Tan, J. (2011). Mesenchymal-stem-cell-based experimental and clinical trials: current status and open questions. Expert Opin. Biol. Ther. *11*, 893–909.

Whitcher, J.P., Srinivasan, M., and Upadhyay, M.P. (2001). Corneal blindness: a global perspective. Bull. World Health Organ. *79*, 214–221.

Yi, X., Li, X., Zhou, Y., Ren, S., Wan, W., Feng, G., and Jiang, X. (2014). Hepatocyte growth factor regulates the TGF-β1-induced proliferation, differentiation and secretory function of cardiac fibroblasts. Int. J. Mol. Med. *34*, 381–390.

Manuscript ID: SC-16-0601.R1
Manuscript Title: Mesenchymal stem cells modulate differentiation of myeloid progenitor cells during inflammation

Dear Dr. Chauhan,

We are pleased to inform you that your manuscript has been accepted for publication in STEM CELLS. The final version of the manuscript is now ready for approval in the submitting author's account on Manuscript Central.

The author who submitted the manuscript now needs to log on to the site at http://mc.manuscriptcentral.com/stemcells and go to the "Manuscripts Accepted for First Look" folder in his or her account to complete the necessary steps before the Editorial Office can schedule the manuscript for publication in both the print version of the Journal and online at www.StemCells.com.

While previewing your materials, please note that your manuscript file must be a Word document, and your figures must be uploaded individually in .eps or .tif format. Tables may be included in the manuscript Word document, or as a separate Word doc. Powerpoint and PDF files will not be processed. While previewing the manuscript, please verify that all author contributions are listed on the title page of the manuscript and that all information concerning author names and affiliated institutions is correct. If your accepted manuscript was a revision, please make sure all red text is converted to black and all underlined text and track changes are removed.

Also, please remember that the Journal allows for only seven figures and tables combined. Anything over this amount must be labeled as supplemental. Please also be sure that your figures meet acceptable resolution requirements specified on the following digital art website: http://cjs.cadmus.com/da/guidelines.jsp#rez. When converting your figure files, you may want to use IrfanView, a recommended graphic program that allows you to save your images as .tif files using LZW compression. This software can be downloaded free at http://www.tucows.com/preview/194967

As a reminder, key words are highly utilized by search engines when ranking search results; therefore, selecting appropriate key words (i.e., search terms) and using them frequently and appropriately in the title, abstract, and article is critical. To improve your article's search engine optimization (SEO), please ensure that: at least 5 relevant key words are carefully selected; the title of your manuscript is short and informative, featuring these key words; the key words are repeated 3-4 times throughout the abstract. These SEO techniques can help boost STEM CELLS's content to high-ranking positions in search results, resulting in greater visibility, readership, and citations for your article.

Lastly, STEM CELLS now features graphical abstracts on our homepage and is published with a graphical Table of Contents (TOC). If you have not already done so, please upload an attractive full color image for the graphical TOC at this time. Please label this image "Graphical Abstract" and upload it as a supplemental file in high resolution .eps or .tif format. Please include the legend for this figure at the end of your manuscript.

We request that you complete these steps in five business days or less to avoid publication delays.

<i>Additional information for optional article enhancements:</i>

<u>Press Release</u>
If you or your institution will be issuing a press release regarding the publication of this manuscript,

please notify us so that we may coordinate the embargo date with our production team.

<u>Social Media and Kudos</u>
In addition to sharing your article on your preferred social media platforms, we encourage our authors to use Kudos, a web-based service that helps to explain, enrich, and share your published work. Free for STEM CELLS authors to improve your article's online discoverability, Kudos also provides a tailored dashboard to measure the effect of your manuscript across a wide range of metrics. To claim your work, please log-in to Wiley Author Services.

<u>Video Highlight</u>
STEM CELLS is now posting video highlights on the Journal homepage. We would like to invite you to submit a video highlight to introduce your soon-to-be published paper. A video highlight is essentially a short video introduction (2-5 minutes) from you that will excite readers' interest in your article. This video supplement will add a new dimension to the work and could draw additional readers. If you would like to create a video highlight for your accepted manuscript, please reply to julie.vo@alphamedpress.com for further information.

On behalf of the Editors and the Editorial Board, we congratulate you on the publication of your important research contributions.

Sincerely,

Jan A. Nolta
Editor-in-Chief
STEM CELLS

![STEM CELLS logo]

Mesenchymal stem cells modulate differentiation of myeloid progenitor cells during inflammation

Journal:	*Stem Cells*
Manuscript ID	SC-16-0601.R1
Wiley - Manuscript Type:	Original Research
Date Submitted by the Author:	n/a
Complete List of Authors:	Amouzegar, Afsaneh; Harvard Medical School, Schepens Eye Research Institute Mittal, Sharad; Harvard Medical School, Schepens Eye Research Institute Sahu, Anuradha; Harvard Medical School, Schepens Eye Research Institute Sahu, Srikant; Harvard Medical School, Schepens Eye Research Institute Chauhan, Sunil; Harvard Medical School, Schepens Eye Research Institute
Keywords:	Immunosuppression, Mesenchymal stem cells, Myeloid cells, Adult stem cells
Journal Section:	Regenerative Medicine
Cell Types:	Mesenchymal Stem Cells
Diseases/Processes/Areas:	Immunomodulation

SCHOLARONE™
Manuscripts

1 **Mesenchymal stem cells modulate differentiation of myeloid progenitor cells**

2 **during inflammation**

3

4 **Running Title: MSCs modulate myeloid progenitor differentiation**

5

6 Afsaneh Amouzegar[1,2], Sharad K. Mittal[1,2], Anuradha Sahu[1], Srikant K. Sahu[1,3], Sunil K.

7 Chauhan[1,2]*

8

9 [1]Schepens Eye Research Institute, Massachusetts Eye and Ear, Boston, MA 02114, USA

10 [2]Department of Ophthalmology, Harvard Medical School, Boston, MA 02114, USA

11 [3]L. V. Prasad Eye Institute, Bhubaneswar, Odisha 751024, India

12

13 **Afsaneh Amouzegar**: collection and assembly of data, data analysis and interpretation,
14 manuscript writing
15 **Sharad K. Mittal**: collection and assembly of data, data analysis and interpretation
16 **Anuradha Sahu**: data analysis and interpretation
17 **Srikant K. Sahu**: data analysis and interpretation
18 **Sunil K. Chauhan**: conception and design, data analysis and interpretation, manuscript writing
19 and final approval of manuscript
20

21

22 ***Correspondence to-**
23 Sunil Chauhan, PhD.
24 Schepens Eye Research Institute
25 Harvard Medical School
26 20 Staniford Street, Boston, MA 02114
27
28
29
30

37

1

38   **Abstract**

39   Mesenchymal stem cells (MSCs) possess distinct immunomodulatory properties and have

40   tremendous potential for use in therapeutic applications in various inflammatory diseases. MSCs

41   have been shown to regulate pathogenic functions of mature myeloid inflammatory cells, such as

42   macrophages and neutrophils. Intriguingly, the capacity of MSCs to modulate differentiation of

43   myeloid progenitors to mature inflammatory cells remains unknown to date. Here, we report the

44   novel finding that MSCs inhibit the expression of differentiation markers on myeloid progenitors

45   under inflammatory conditions. We demonstrate that the inhibitory effect of MSCs is dependent

46   on direct cell-cell contact and that this intercellular contact is mediated through interaction of

47   CD200 expressed by MSCs and CD200R1 expressed by myeloid progenitors. Further, using an

48   injury model of sterile inflammation, we show that MSCs promote myeloid progenitor

49   frequencies and suppress infiltration of inflammatory cells in the inflamed tissue. We also find

50   that downregulation of CD200 in MSCs correlates with abrogation of their immunoregulatory

51   function. Collectively, our study provides unequivocal evidence that MSCs inhibit differentiation

52   of myeloid progenitors in the inflammatory environment via CD200-CD200R1 interaction.

1
2
3
4
5
6
7
8
9
10
11
12
13
14
15
16
17
18
19
20
21
22
23
24
25
26
27
28
29
30
31
32
33
34
35
36
37
38
39
40
41
42
43
44
45
46
47
48
49
50
51
52
53
54
55
56
57
58
59
60

53 **Introduction**

54 During hematopoiesis, myeloid lineage-committed progenitors derived from hematopoietic stem

55 cells (HSCs) in the bone marrow give rise to mature myeloid cells such as macrophages and

56 neutrophils [1]. The bone marrow is also home to non-hematopoietic stromal cells such as

57 mesenchymal stem cells (MSCs), which, in addition to providing a niche and trophic support for

58 HSCs, maintain hematopoiesis by sustaining a part of the HSC population in an undifferentiated

59 quiescent state through release of soluble factors and intercellular interactions [2, 3].

60   Acute inflammatory stresses lead to deviation of hematopoiesis toward preferential

61 induction of committed myeloid progenitors and their subsequent differentiation into mature

62 macrophages and neutrophils [4]. The highly proliferative capacity of myeloid progenitors plays

63 a central role in inflammation-induced myelopoeisis, restoring consumed macrophages and

64 neutrophils at the site of inflammation [5]. Despite the critical role of mature myeloid cells in

65 host defense and resolution of inflammation, excessive innate immune response can have

66 deleterious effects on tissue homeostasis and lead to undesired tissue damage.

67   In addition to supporting hematopoiesis, MSCs are characterized by their self-renewal

68 and multilineage differentiation potential and unique immunoregulatory properties [6]. Studies

69 on the interaction between MSCs and immune cells have shown that MSCs can regulate

70 functions of mature innate immune cells, including polarization of inflammatory macrophages

71 into an anti-inflammatory phenotype and enhancement of the phagocytic capacity of neutrophils

72 [7, 8].

73   Although much is known about the regulatory role of MSCs on function of mature

74 myeloid cells, information regarding potential regulatory interactions between MSCs and

75 myeloid progenitor cells is lacking. Given the central role of myeloid progenitors in

3

76   inflammation, regulating differentiation of these precursors into pathogenic myeloid cells could

77   effectively inhibit inflammatory response at an earlier stage. In this study, we sought to

78   determine whether MSCs can inhibit the differentiation of myeloid progenitors into mature

79   inflammatory cells during inflammation. Specifically, we demonstrate that MSCs inhibit

80   differentiation of myeloid progenitors and maintain these cells in an immature state. Using both

81   *in vitro* co-culture assays and an *in vivo* model of injury-induced sterile inflammation, we show

82   that MSCs exert immunoregulatory effects on myeloid progenitors in a cell-cell contact

83   dependent manner – a process mediated through CD200-CD200R1 interaction.

4

84　**Materials and Methods**

85　**Animals**

86　Six- to eight-week-old male C57BL/6 mice (Charles River Laboratories, Wilmington, MA,

87　USA) were used in the experiments. Mice were kept in a pathogen-free environment at the

88　Schepens Eye Research Institute Animal Facility. The protocol was approved by the Schepens

89　Eye Research Institute Animal Care and Use Committee, and all animals were treated in

90　accordance with the ARVO Statement for the Use of Animals in Ophthalmic and Vision

91　Research.

92　**Isolation, expansion, and characterization of mesenchymal stem cells**

93　Bone marrow was harvested from femur bones of euthanized C57BL/6 mice. Using the

94　previously described plastic adherence method of MSC cultivation [9, 10], bone marrow cells

95　were cultured at 37°C in murine MesenCult basal medium and supplement (Stem Cell

96　Technologies, Vancouver, BC, Canada). Cells were passaged at every three to five days

97　intervals. Before using in experiments, MSCs from third passage were characterized

98　phenotypically for the expression of MSC markers ($CD45^-CD34^-SCA1^+CD29^+$) using flow

99　cytometry, and functionally by in vitro differentiation using adipocytes using MesenCult

100　adipogenic stimulatory supplements (Stem Cell Technologies). Oil-red-O (Sigma-Aldrich, St.

101　Louis, MO) staining was used to confirm the differentiation of MSCs into the adipocytes. MSCs

102　from third passage were used in both in vitro and in vivo experiments.

103

104　**Myeloid progenitor cell characterization and isolation**

105　Single cell suspensions from spleen, bone marrow, and draining submandibular lymph nodes

106　harvested from C57BL/6 mice were stained with fluorochrome-conjugated monoclonal

5

107   antibodies to CD14 (#123308), CD11b (#101210), CD34 (#119307), c-kit (#105817), and

108   FcγRII/III (#101327) (Biolegend, San Diego, CA, USA) for characterization of myeloid

109   progenitors. Due to higher frequencies of myeloid progenitors in the spleen, $CD14^+CD11b^-$

110   progenitors were then isolated from the spleen by flow sorting (MoFlo XDP, Beckman Coulter).

111   Purity of isolated myeloid progenitors (>95%) was determined by flow cytometry. Isolated

112   spleen-derived progenitors were characterized for the expression of progenitor and mature

113   myeloid cell markers before being used in in vitro experiments, as described later in Flow

114   cytometry method.

Co-culture and transwell assays

116   Isolated spleen-derived myeloid progenitors (2×10^5 cells) were cultured with or without in-vitro

117   expanded MSCs (4×10^4 cells) for 72 hours in the presence of 100ng/mL IFNγ, 100 ng/mL IL-1β,

118   or 10 ng/mL GMCSF (Biolegend, San Diego, CA, USA) as inflammatory or hematopoietic

119   growth factor stimuli. For the indirect co-culture, MSCs were first cultured in a monolayer on 6.5

120   mm transwell inserts with 0.4 μm pore size (Corning, NY, USA) and then co-cultured with

121   isolated myeloid progenitors at the ratio of 1:5 MSCs to myeloid progenitors in the presence of

122   100ng/mL IFNγ for 72 hours.

shRNA transfection

124   MSCs ($1.5x10^6$ cells) were plated in a 75 cm^2 flask and incubated for 18-24 hours to reach to 60-

125   70% confluency. The cells were then washed and transfected with CD200-specific or non-

126   specific control shRNA using transfection reagent in shRNA transfection media according to the

127   protocol suggested by the manufacturer (Santa Cruz Biotechnology, Dallas, TX). After overnight

128   incubation, transfection media was replaced with normal MSC growth culture media and cells

6

129　were cultured for additional 2 days. Knockdown efficiency of shRNA was validated by real-time

130　PCR using CD200-specific primers 48 hours after transfection (Supplement Fig. S4).

Corneal injury model

132　Corneal injury was induced in mice as described previously [11, 12]. Briefly, Mice were

133　anesthetized by intraperitoneal injection of Ketamine and Xylazine. Central cornea of deeply

134　anesthetized mice was marked by a 2mm trephine. Using the tip of a hand-held motor brush

135　(AlgerBrush II, Alger Company Inc., Lago Vista, TX), total corneal epithelium and anterior

136　stroma were removed mechanically to create corneal injury. Upon completion of the procedure,

137　triple antibiotic ointment was applied to the injured eyes, and a subcutaneous injection of

138　Buprenorphine was given to mice to minimize injury-induced pain. To study the therapeutic

139　effect of MSCs on corneal inflammation, mice were randomly divided into injury only or MSC

140　(wild-type or CD200 shRNA)-recipient groups, with $n=5$ in each group. In vitro expanded and

141　characterized MSCs or CD200 shRNA-treated MSCs $(0.5\times10^6$ cells suspended in 100μL sterile

142　saline) were injected into the tail veins of mice 1-hour post injury. Mice were euthanized 48

143　hours post injury to collect corneas for flow cytometry, real-time PCR, and fluorescence

144　microscopy analyses as described later.

Flow cytometry

146　Flow cytometry was performed to characterize the phenotype of in vitro expanded MSCs and

147　myeloid progenitors, to evaluate in vitro differentiation of myeloid progenitors, and to quantify

148　the frequencies of $CD45^+$ and myeloid progenitors in the cornea. Cultured MSCs in single cell

149　suspension were stained with conjugated monoclonal antibodies to CD45 (#103115), CD34

150　(#119307), Sca-1 (#108107), CD29 (#102207), CD11b (#101210), c-Kit (#105817), CD105

151　(#120407), CD31 (#102407), and CD200 (#123807). Single cell suspensions were prepared from

7

152   bone marrow, spleen, and draining submandibular lymph nodes and were stained with

153   conjugated monoclonal antibodies to CD14 (#123308), CD11b (#101235), CD34 (#119307), c-

154   kit (#105817), FcγRII/III (#101327), Ly6G (#127627), Ly6C (#128007), and CD200R1

155   (#123907). Single cell suspensions of cultured myeloid progenitors were stained with conjugated

156   monoclonal antibodies to CD11b (#101210), Ly6G (#127627) and CD11c (#117329). Corneas

157   were harvested 48 hours post injury and were digested in RPMI media (Lonza, Walkersville,

158   MD) containing 2 mg/mL collagenase type IV (Sigma-Aldrich, St. Louis, MO) and 2 mg/mL

159   DNase I (Roche, Basel, Switzerland) for 45 minutes at 37 °C and then filtered through a 70-μm

160   cell strainer. Corneal single cell suspensions were then stained with conjugated monoclonal

161   antibodies to CD45 (#103133), CD34 (#119307), CD14 (#123308) and CD11b (#101210). All

162   the antibodies with their matched isotype controls were purchased from Biolegend (San Diego,

163   CA, USA). Stained cells were analyzed using an LSR II flow cytometer (BD Biosciences, San

164   Jose, CA, USA).

165   **RNA isolation, RT-PCR, and quantitative real-time PCR**

166   Corneas were harvested at 48 hours post injury from each group, and mRNA was isolated using

167   the RNeasy Micro Kit (Qiagen, Germantown, MD, USA). Isolated RNA was reverse transcribed

168   into cDNA using oligo (dT) primer and Superscript TM III (Invitrogen, Grand Island, NY,

169   USA). Real-time PCR was performed using Taqman Universal PCR Mastermix and

170   preformulated primers for PDL-1 (Mm00452054_m1), VTCN-1 (Mm00628552_m1), Ceacam-1

171   (Mm04204476_m1), CD200 (Mm00487740_m1), IL-1β (Mm00434228_m1), and

172   glyceraldehype-3-phosphate dehydrogenase (GAPDH, Mm99999915_g1) (Thermofisher

173   Scientific, Waltham, MA, USA). The results were analyzed by the comparative threshold cycle

174   method and normalized to GAPDH as an internal control.

175 **Immunofluorescence and histopathology**

176 Freshly excised corneas were washed in PBS and fixed with 4% paraformaldehyde for 20

177 minutes and permeabilized with 0.5% Triton X-100 for 10 minutes. Whole corneas were then

178 immunostained with FITC-conjugated anti-CD14 (#123308) and PE-conjugated anti-CD11b

179 (#101207) (Biolegend (San Diego, CA, USA) overnight at 4°C to detect myeloid progenitors and

180 mounted onto slides with mounting medium (Vector Laboratories, Burlingame, CA, USA) and

181 visualized using a confocal microscope (Leica TCS-SP5; Buffalo Grove, IL, USA) at ×20

182 magnification. Corneal sections fixed in 4% paraformaldehyde were stained with hematoxylin

183 and eosin. Images were obtained using a bright field microscope (Nikon Eclipse E800; Melville,

184 NY, USA) at ×20 magnification.

185 **Statistical analysis**

186 A two-tailed Student's *t-test* was performed and P values <0.05 were regarded as statistically

187 significant. Results are presented as the mean ± standard error of the mean (SEM) of at least

188 three independent experiments. Samples sizes were estimated on the basis of previous

189 experimental studies on corneal injury and inflammation [10, 13].

9

190 **Results**

191 **Characterization of myeloid progenitor cells**

192 As immune cells are primarily developed in lymphoid organs, single cell suspensions from bone

193 marrow, spleen, and submandibular lymph nodes were immunostained for flow cytometry

194 analysis as per the gating strategy shown in Supplement Figure S1. First, a population of

195 $CD14^+CD11b^-$ cells was identified (Fig. 1A) and gated for further characterization and for

196 examining the expression of progenitor cell markers, including CD34, c-Kit, and FcγRII/III, as

197 well as the mature myeloid cell markers, Ly6G granulocytic marker and Ly6C monocytic marker

198 (Fig. 1B). Majority of $CD14^+CD11b^-$ cells (~80%) were positive for the expression of CD34, c-

199 Kit and FcγRII/III progenitor markers, and all (~99%) were negative for Ly6G and Ly6C mature

200 myeloid cell markers (Fig. 1B). Based on our results, we estimate that myeloid progenitors

201 $(CD34^+c\text{-}Kit^+Fc\gamma RII/III^+CD14^+ CD11b^-Ly6G^-Ly6C^-)$ constitute 4.8±1.09% of bone marrow

202 cells, 8.7±0.29% of splenocytes, and 4.1±0.31% of lymph node cells (Fig. 1C).

203

204 **MSCs inhibit differentiation of myeloid progenitor cells in vitro**

205   Bone marrow-derived MSCs were cultured and characterized as per criteria defined by The

206 International Society for Cellular Therapy [9, 10]. MSCs were expanded using the plastic

207 adherence method, and were characterized phenotypically for positive expression of SCA1 and

208 CD29 and negative expression of CD45 and CD34 surface markers, and functionally by their

209 ability to differentiate into adipocytes (Fig. 2A). Next, sorted myeloid progenitor cells were

210 cultured with or without MSCs in the presence or absence of inflammatory or hematopoietic

211 growth stimuli such as IFNγ, IL-1β or GMCSF, which have been implicated in myeloid cell

212 differentiation[14-16]. After stimulation with IFNγ, IL-1β or GMCSF, expression of mature

213 myeloid cell markers, including CD11b (marker for macrophages; also known as macrophage-1

214 antigen [Mac-1]) and Ly6G (marker for granulocytes) was investigated using flow cytometry to

215 assess progenitor cell differentiation. Our data showed that upon stimulation with IFNγ, myeloid

216 progenitors acquire high expression of both CD11b and Ly6G. Further analysis demonstrated a

217 significant reduction (55%) in expression of CD11b by myeloid progenitor cells cultured with

218 MSCs in contrast to those cultured without MSCs (MFI 4.15 ±1.04 vs. 9.2 ±1.6; p= 0.000065)

219 (Fig. 2B), and a significant 58% suppression in expression of Ly6G in progenitors cultured with

220 MSCs compared to progenitors cultured without MSCs (MFI 9.9 ± 0.75 vs. 23.02 ±1.14, p=

221 0.0000013) (Fig. 2C). Strikingly, our data that myeloid progenitors fail to express CD11c in the

222 steady state or upon stimulation, suggest that these myeloid progenitors do not differentiate into

223 dendritic cells (Supplement Fig. S2). Similar to effects of IFNγ on myeloid progenitors,

224 stimulation with IL-1β and GMCSF also resulted in selective expression of CD11b by myeloid

225 progenitors, which was significantly suppressed in myeloid progenitors co-cultured with MSCs

226 (Supplement Fig. S3). Taken together, these data suggest that MSCs suppress acquisition of

227 differentiation markers by myeloid progenitors and maintain these cells in an immature state in

228 an inflammatory environment.

229

MSCs interact with myeloid progenitors in a cell-cell contact-dependent manner

231 To delineate whether the inhibitory effect of MSCs on myeloid progenitor differentiation was

232 through direct cell-cell contact or by MSC-secreted soluble factors, MSCs were either cultured in

233 direct contact with isolated myeloid progenitors, or were first plated into transwell inserts and

234 then cultured with myeloid progenitor cells with IFNγ stimulation. Expression of CD11b surface

235 marker was assessed using flow cytometry. As shown in Figure 3A, MSCs that were cultured

11

236   directly with myeloid progenitors significantly suppressed acquisition of CD11b differentiation

237   marker by these cells. However, MSCs in the transwell chamber system failed to suppress

238   CD11b expression by myeloid progenitors, suggesting that the suppressive function of MSCs is

239   dependent on direct cell-cell contact rather than secretion of soluble factors by MSCs. To further

240   explore the molecular mechanism underlying such contact-dependency, we investigated the

241   expression of following cell membrane-bound inhibitory molecules by MSCs using real time

242   PCR: programmed death-ligand 1 (PD-L1), a transmembrane protein, which delivers inhibitory

243   signals to immune cells upon binding with PD-1 expressed by T cells and activated monocyte; v-

244   set domain containing T cell activation inhibitor 1 (VTCN-1) or B7-H4, a transmembrane protein

245   that negatively regulates the function of T cells and neutrophils [17]; CD200 (OX2), a

246   transmembrane glycoprotein that inhibits function of myeloid immune cells [18]; and

247   carcinoembryonic antigen-related cell adhesion molecule 1 (Ceacam-1), a cell adhesion molecule

248   involved in contact-dependent regulation of the innate and adaptive immune responses [19] (Fig.

249   3B). Significantly higher mRNA expression of CD200 compared to other molecules prompted us

250   to speculate that CD200 may be the critical ligand mediating the immunoregulatory function of

251   MSCs. Our data further demonstrated that MSCs significantly upregulate their expression of

252   CD200 in the inflammatory environment (Fig. 3C). Using flow cytometry, we also confirmed

253   protein expressions of CD200 on MSCs and its receptor, CD200R1 on myeloid progenitor cells

254   (Fig. 3D & E).

255

256   **MSCs inhibit differentiation of myeloid progenitors via CD200-CD200R1 interaction**

257   Next, to investigate the role of CD200 in mediating the immunoregulatory function of MSCs in

258   vitro, functional expression of CD200 on MSCs was silenced using CD200-shRNA (Supplement

12

259   Fig. S4). Control-shRNA or CD200-shRNA treated MSCs were then cultured with myeloid

260   progenitors in the presence of IFNγ. Our data regarding expression of CD11b demonstrated that

261   CD200-shRNA-treated MSCs had 22% less ability in suppressing myeloid progenitor

262   differentiation compared to control-shRNA-treated MSCs (p=0.008) (Fig. 3F). Compromised

263   ability of CD200-shRNA MSCs to suppress myeloid progenitor acquisition of CD11b suggests

264   that expression of CD200 by MSCs is critical for their inhibitory function on myeloid progenitor

265   differentiation.

266

267   CD200 expression in MSCs is indispensable for suppression of inflammation and

268   accumulation of undifferentiated myeloid progenitors in the inflamed tissue

269   Lastly, we chose a sterile inflammation *in vivo* model of mouse eye injury – a well-established

270   system to study inflammation [13, 20] – to confirm the immunoregulatory effect of MSCs on

271   myeloid progenitors. This well-characterized model provides an excellent system to study

272   inflammation. Simple anatomy of the eye and its paucity of resident immune cells facilitate study

273   of recruited immune cells and their contribution to the inflammatory response [21]. As

274   demonstrated previously [10, 22], we show that MSCs administered systemically home

275   specifically to the injured cornea (Supplement Fig. S5). Interestingly, similar to the bone

276   marrow, spleen and lymph node, we identified a population of $CD34^+CD14^+CD11b^-$ myeloid

277   progenitors in the cornea (Fig. 4A). Our immunofluorescence microscopy results also confirmed

278   the presence of $CD14^+CD11b^-$ progenitors primarily in the stromal layer of cornea (Fig. 4B).

279   Similar to lymphoid tissue-derived progenitors, upon stimulation with IFNγ, sorted corneal

280   myeloid progenitors expressed CD11b, and MSCs suppressed their acquisition of CD11b *in vitro*

281   (Supplement Fig. S6). To determine the effect of systemic administration of MSCs on myeloid

13

282   progenitor cell frequencies and tissue inflammation, mice were intravenously injected with

283   control-shRNA or CD200-shRNA-treated MSCs 1 hour after corneal injury induction, followed

284   by harvesting of corneas 48 hours post-injury (Fig. 4C). Our flow cytometry data demonstrated

285   that normal (control-shRNA-treated) MSCs led to a 5-fold increase in the frequencies of corneal

286   myeloid progenitors, while CD200-shRNA-treated MSCs failed to do so, suggesting that MSC

287   expression of CD200 is important for expansion of myeloid progenitor cell frequencies in the

288   inflamed tissue (Fig. 4E). Similar to our previous findings on the anti-inflammatory effect of

289   MSCs in the inflamed tissue, our data demonstrated that normal (control-shRNA-treated) MSCs,

290   but not CD200-silenced MSCs, have a significant suppressive effect on tissue inflammation as

291   evidenced by reduced frequencies of $CD45^+$ cells (Fig. 4D), decreased expression of

292   inflammatory cytokine IL-1β (Fig. 4G) and less inflammatory cell infiltration in the corneal

293   stroma (Fig. 4F) compared to untreated mice with corneal injury. These findings strongly suggest

294   that MSCs suppress tissue inflammation by reducing inflammatory cell infiltration and by

295   expanding frequencies of myeloid progenitor cells through a CD200-dependent mechanism.

1
2
3
4
5
6
7
8
9
10
11
12
13
14
15
16
17
18
19
20
21
22
23
24
25
26
27
28
29
30
31
32
33
34
35
36
37
38
39
40
41
42
43
44
45
46
47
48
49
50
51
52
53
54
55
56
57
58
59
60

296 **Discussion**

297 The current study ascribes a novel immunoregulatory function for MSCs on myeloid progenitor

298 cell differentiation. Our data indicate that MSCs inhibit differentiation of myeloid progenitor

299 cells in an inflammatory environment through direct cell-cell contact. Furthermore, we

300 demonstrate that this intercellular contact is mediated by CD200-CD200R1 interaction, and that

301 CD200 expression by MSCs is indispensable for inhibition of myeloid progenitor differentiation

302 and suppression of tissue inflammation.

303 Myeloid progenitors are precursors of mature myeloid cells, critical effector cells in

304 innate immune response. Upregulation of pro-inflammatory cytokines such as IFNγ, IL1β and

305 TNFα during inflammation activates steady state progenitors in the bone marrow to differentiate

306 into myeloid effector cells [4, 23]. Myeloid progenitors are primarily found in the bone marrow

307 and cord blood [24]. Some studies have demonstrated the presence of undifferentiated

308 monocytes and DC precursors in non-bone marrow tissues such as spleen [25, 26]. Our findings

309 demonstrate a population of myeloid progenitors, which in addition to the bone marrow are also

310 present in peripheral lymphoid tissues, including spleen and lymph nodes. These progenitors

311 express high levels of CD34, CD14, c-Kit and FcγRII/III progenitor markers, which makes them

312 phenotypically similar to early myeloid progenitors such as common myeloid progenitors

313 (CMPs) and granulocyte/macrophage progenitors (GMPs) [27, 28]. CMPs are thought to be

314 precursors of common DC progenitors, which eventually give rise to DCs [27]. Our data,

315 however, demonstrate that the myeloid progenitors identified do not express the DC marker

316 CD11c in the steady or activated states, suggesting that these cells are not DC precursors. Rather,

317 these progenitors acquire high levels of CD11b and Ly6G myeloid markers in the inflammatory

15

318   milieu, suggesting these myeloid progenitors are phenotypically closer to GMPs that give rise to

319   macrophages and granulocytes [1, 27, 29].

320   Interestingly, we find that MSCs inhibit acquisition of CD11b and Ly6G differentiation

321   markers on myeloid progenitors. MSCs have been shown to interact with cells of both innate and

322   adaptive immunity [30]. Recent reports on the interaction of MSCs with DC precursors have

323   demonstrated that MSCs inhibit differentiation of peripheral blood-derived CD14$^+$ monocytes to

324   mature DCs [31, 32]. Here, our data show that MSCs negatively regulate both bone marrow- and

325   peripheral lymphoid tissue-resident myeloid progenitors. MSCs maintain these cells in an

326   undifferentiated quiescent state and further prevent their differentiation into inflammatory cells.

327   MSCs primarily exert their immunoregulatory effects through secretion of paracrine factors such

328   as IDO, IL-10, TGF-β and TSG6 [33, 34]. In contrast, we find that MSCs inhibit differentiation

329   of myeloid progenitors mainly through direct cell-cell contact. The results of our study

330   demonstrate that silencing of CD200 expression in MSCs abrogates their ability to suppress

331   myeloid progenitor cell differentiation, suggesting that CD200-CD200R1 interaction is critical

332   for MSCs to exert their immunoregulatory effect. CD200 or Ox-2 is a transmembrane

333   glycoprotein, which binds to its receptor CD200R1 [35]. The CD200R family of receptors

334   consists of 4 isoforms [36], among which CD200R1 is mainly expressed by myeloid cells and T

335   cells [35, 37]. CD200-CD200R1 pathway plays a central role in regulation of innate immune

336   system by inhibiting myeloid cell activation [38, 39]. We show that bone marrow-derived MSCs

337   constitutively express CD200, and significantly upregulate CD200 expression in response to

338   inflammatory stimuli. These results are consistent with previous studies which demonstrated that

339   IFNγ in particular induces CD200 expression in bone marrow-derived stromal cells [40] .

340   Finally, the functional relevance of MSC regulation of myeloid progenitor cell

341   differentiation during inflammation was tested using a standardized mouse cornea model of

342   sterile injury [10, 41]. Similar to the bone marrow, spleen and lymph nodes, we have identified

343   myeloid progenitors residing in the cornea. MSCs have been shown to migrate to the sites of

344   inflammation and promote wound repair [42, 43]. Previously, we showed that systemically

345   administered MSCs home to the inflamed eye, and accelerate wound healing [10, 22]. Here, we

346   show that MSCs suppress infiltration of inflammatory cells and increase the frequencies of

347   corneal myeloid progenitors. Consistent with our *in vitro* findings, systemically administered

348   CD200-shRNA-treated MSCs lose their ability to suppress differentiation of myeloid progenitors

349   and tissue inflammation. The increase in myeloid progenitor frequencies at the inflamed site

350   could be the result of MSC-mediated expansion of corneal resident myeloid progenitors, or due

351   to MSCs inhibiting differentiation of recruited myeloid progenitors from the bone marrow. Early

352   myeloid progenitors have recently been identified as immunosuppressive cells that are capable of

353   inhibiting T cell proliferation [44]. If MSCs promote recruitment of myeloid progenitors to the

354   inflamed tissue, suppression of inflammation could be the cumulative result of MSC-and

355   myeloid progenitor-mediated regulation of the immune response. However, we acknowledge that

356   further experiments will be needed to elucidate the exact mechanism by which MSCs promote

357   myeloid progenitor frequencies at the site of inflammation.

1
2
3
4
5
6
7
8
9
10
11
12
13
14
15
16
17
18
19
20
21
22
23
24
25
26
27
28
29
30
31
32
33
34
35
36
37
38
39
40
41
42
43
44
45
46
47
48
49
50
51
52
53
54
55
56
57
58
59
60

358 **Conclusion**

359 In conclusion, our findings provide new insight into the immunoregulatory effect of MSCs on

360 myeloid progenitor cell differentiation. Herein, we show that MSCs suppress inflammation not

361 only by regulating inflammatory cell infiltration, but also by preventing differentiation of early

362 myeloid precursors into inflammatory cells. Our data further supports a critical role for CD200

363 expressed by MSCs in regulating function of myeloid progenitors and thus inhibiting

364 inflammatory response. These observations could provide a framework for the development of

365 potential CD200-based therapeutics that could effectively modulate the generation of innate

366 immune cells and inhibit inflammation at early stage.

1
2
3
4
5
6
7
8
9
10
11
12
13
14
15
16
17
18
19
20
21
22
23
24
25
26
27
28
29
30
31
32
33
34
35
36
37
38
39
40
41
42
43
44
45
46
47
48
49
50
51
52
53
54
55
56
57
58
59
60

372 **References:**

373 1. Kondo M. Lymphoid and myeloid lineage commitment in multipotent hematopoietic
374 progenitors. **Immunol Rev**. 2010;238:37-46.

375 2. Li T, Wu Y. Paracrine molecules of mesenchymal stem cells for hematopoietic stem cell
376 niche. **Bone Marrow Res**. 2011;2011:353878.

377 3. da Silva CL, Goncalves R, dos Santos F et al. Dynamic cell-cell interactions between
378 cord blood haematopoietic progenitors and the cellular niche are essential for the
379 expansion of CD34+, CD34+CD38- and early lymphoid CD7+ cells. **J Tissue Eng**
380 **Regen Med**. 2010;4:149-158.

381 4. Maltby S, Hansbro NG, Tay HL et al. Production and differentiation of myeloid cells
382 driven by proinflammatory cytokines in response to acute pneumovirus infection in mice.
383 **J Immunol**. 2014;193:4072-4082.

384 5. King KY, Goodell MA. Inflammatory modulation of HSCs: viewing the HSC as a
385 foundation for the immune response. **Nat Rev Immunol**. 2011;11:685-692.

386 6. Uccelli A, Moretta L, Pistoia V. Mesenchymal stem cells in health and disease. **Nat Rev**
387 **Immunol**. 2008;8:726-736.

388 7. Hall SR, Tsoyi K, Ith B et al. Mesenchymal stromal cells improve survival during sepsis
389 in the absence of heme oxygenase-1: the importance of neutrophils. **Stem Cells**.
390 2013;31:397-407.

391 8. Bernardo ME, Fibbe WE. Mesenchymal stromal cells: sensors and switchers of
392 inflammation. **Cell Stem Cell**. 2013;13:392-402.

393 9. Dominici M, Le Blanc K, Mueller I et al. Minimal criteria for defining multipotent
394 mesenchymal stromal cells. The International Society for Cellular Therapy position
395 statement. **Cytotherapy**. 2006;8:315-317.

396 10. Lan Y, Kodati S, Lee HS et al. Kinetics and function of mesenchymal stem cells in
397 corneal injury. **Invest Ophthalmol Vis Sci**. 2012;53:3638-3644.

398 11. Basu S, Hertsenberg AJ, Funderburgh ML et al. Human limbal biopsy-derived stromal
399 stem cells prevent corneal scarring. **Sci Transl Med**. 2014;6:266ra172.

400 12. Mittal SK, Omoto M, Amouzegar A et al. Restoration of Corneal Transparency by
401 Mesenchymal Stem Cells. **Stem Cell Reports**. 2016;7:583-590.

402 13. Lee RH, Yu JM, Foskett AM et al. TSG-6 as a biomarker to predict efficacy of human
403 mesenchymal stem/progenitor cells (hMSCs) in modulating sterile inflammation in vivo.
404 **Proc Natl Acad Sci U S A**. 2014;111:16766-16771.

405 14. de Bruin AM, Voermans C, Nolte MA. Impact of interferon-gamma on hematopoiesis.
406 **Blood**. 2014;124:2479-2486.

407 15. Orelio C, Haak E, Peeters M et al. Interleukin-1-mediated hematopoietic cell regulation
408 in the aorta-gonad-mesonephros region of the mouse embryo. **Blood**. 2008;112:4895-
409 4904.

410 16. Metcalf D. Hematopoietic cytokines. **Blood**. 2008;111:485-491.

411 17. Ceeraz S, Nowak EC, Noelle RJ. B7 family checkpoint regulators in immune regulation
412 and disease. **Trends Immunol**. 2013;34:556-563.

413   18.   Wright GJ, Cherwinski H, Foster-Cuevas M et al. Characterization of the CD200 receptor
414   family in mice and humans and their interactions with CD200. **J Immunol**.
415   2003;171:3034-3046.

416   19.   Gray-Owen SD, Blumberg RS. CEACAM1: contact-dependent control of immunity. **Nat
417   Rev Immunol**. 2006;6:433-446.

418   20.   Oh JY, Roddy GW, Choi H et al. Anti-inflammatory protein TSG-6 reduces
419   inflammatory damage to the cornea following chemical and mechanical injury. **Proc Natl
420   Acad Sci U S A**. 2010;107:16875-16880.

421   21.   Gronert K. Ocular Inflammation Models. In: Serhan CN WP, Gilroy DW, ed.
422   Fundamentals of Inflammation: Cambridge University Press; 2010:413-426.

423   22.   Omoto M, Katikireddy KR, Rezazadeh A et al. Mesenchymal stem cells home to
424   inflamed ocular surface and suppress allosensitization in corneal transplantation. **Invest
425   Ophthalmol Vis Sci**. 2014;55:6631-6638.

426   23.   Takizawa H, Boettcher S, Manz MG. Demand-adapted regulation of early hematopoiesis
427   in infection and inflammation. **Blood**. 2012;119:2991-3002.

428   24.   Lee J, Breton G, Oliveira TY et al. Restricted dendritic cell and monocyte progenitors in
429   human cord blood and bone marrow. **J Exp Med**. 2015;212:385-399.

430   25.   Hey YY, O'Neill HC. Murine spleen contains a diversity of myeloid and dendritic cells
431   distinct in antigen presenting function. **J Cell Mol Med**. 2012;16:2611-2619.

432   26.   Swirski FK, Nahrendorf M, Etzrodt M et al. Identification of splenic reservoir monocytes
433   and their deployment to inflammatory sites. **Science**. 2009;325:612-616.

434   27.   Akashi K, Traver D, Miyamoto T et al. A clonogenic common myeloid progenitor that
435   gives rise to all myeloid lineages. **Nature**. 2000;404:193-197.

436   28.   Manz MG, Miyamoto T, Akashi K et al. Prospective isolation of human clonogenic
437   common myeloid progenitors. **Proc Natl Acad Sci U S A**. 2002;99:11872-11877.

438   29.   Hettinger J, Richards DM, Hansson J et al. Origin of monocytes and macrophages in a
439   committed progenitor. **Nat Immunol**. 2013;14:821-830.

440   30.   Chen X, Armstrong MA, Li G. Mesenchymal stem cells in immunoregulation. **Immunol
441   Cell Biol**. 2006;84:413-421.

442   31.   Jiang XX, Zhang Y, Liu B et al. Human mesenchymal stem cells inhibit differentiation
443   and function of monocyte-derived dendritic cells. **Blood**. 2005;105:4120-4126.

444   32.   Nauta AJ, Kruisselbrink AB, Lurvink E et al. Mesenchymal stem cells inhibit generation
445   and function of both CD34+-derived and monocyte-derived dendritic cells. **J Immunol**.
446   2006;177:2080-2087.

447   33.   Choi H, Lee RH, Bazhanov N et al. Anti-inflammatory protein TSG-6 secreted by
448   activated MSCs attenuates zymosan-induced mouse peritonitis by decreasing TLR2/NF-
449   kappaB signaling in resident macrophages. **Blood**. 2011;118:330-338.

450   34.   Kyurkchiev D, Bochev I, Ivanova-Todorova E et al. Secretion of immunoregulatory
451   cytokines by mesenchymal stem cells. **World J Stem Cells**. 2014;6:552-570.

452   35.   Wright GJ, Cherwinski H, Foster-Cuevas M et al. Characterization of the CD200 receptor
453   family in mice and humans and their interactions with CD200. **J Immunol**.
454   2003;171:3034-3046.

21

455   36.   Gorczynski R, Chen Z, Kai Y et al. CD200 is a ligand for all members of the CD200R
456   family of immunoregulatory molecules. **J Immunol**. 2004;172:7744-7749.

457   37.   Wright GJ, Puklavec MJ, Willis AC et al. Lymphoid/neuronal cell surface OX2
458   glycoprotein recognizes a novel receptor on macrophages implicated in the control of
459   their function. **Immunity**. 2000;13:233-242.

460   38.   Jenmalm MC, Cherwinski H, Bowman EP et al. Regulation of myeloid cell function
461   through the CD200 receptor. **J Immunol**. 2006;176:191-199.

462   39.   Nathan C, Muller WA. Putting the brakes on innate immunity: a regulatory role for
463   CD200? **Nat Immunol**. 2001;2:17-19.

464   40.   Najar M, Raicevic G, Jebbawi F et al. Characterization and functionality of the CD200-
465   CD200R system during mesenchymal stromal cell interactions with T-lymphocytes.
466   **Immunol Lett**. 2012;146:50-56.

467   41.   Basu S, Hertsenberg AJ, Funderburgh ML et al. Human limbal biopsy-derived stromal
468   stem cells prevent corneal scarring. **Sci Transl Med**. 2014;6:266ra172.

469   42.   Karp JM, Leng Teo GS. Mesenchymal stem cell homing: the devil is in the details. **Cell
470   Stem Cell**. 2009;4:206-216.

471   43.   Hong HS, Lee J, Lee E et al. A new role of substance P as an injury-inducible messenger
472   for mobilization of CD29(+) stromal-like cells. **Nat Med**. 2009;15:425-435.

473   44.   Pu S, Qin B, He H et al. Identification of early myeloid progenitors as
474   immunosuppressive cells. **Sci Rep**. 2016;6:23115.

475

1
2
3
4
5
6
7
8
9
10
11
12
13
14
15
16
17
18
19
20
21
22
23
24
25
26
27

476   **Figure legends**

477

478   **Figure 1. Frequencies and phenotypic characterization of myeloid progenitor cells. A.**

479   Representative flow cytometric dot plots showing gating strategy for selecting CD14$^+$CD11b$^-$

480   cells in the bone marrow, spleen, and submandibular lymph nodes. **B.** Representative flow

481   cytometric histograms demonstrating the expression of progenitor markers CD34, c-Kit and

482   FcγRII/III, myeloid marker CD11b, monocytic marker Ly6C, and granulocytic marker Ly6G by

483   CD14$^+$CD11b$^-$ cells. **C.** Bar chart comparing the frequencies of myeloid progenitors in the bone

484   marrow, spleen and lymph node as analyzed by flow cytometry. Representative data from 3

485   independent experiments are shown and each experiment consisted of 5 animals. Data is

486   represented as mean ± SEM.

487   **Figure 2. MSCs inhibit differentiation of myeloid progenitor cells in vitro. A.** *Left Panel:*

488   Expansion and characterization of MSCs. Microscopic images of MSCs cultured in MSC or

489   adipogenic media. Oil-Red-O staining after 2 weeks showed red colored fat vacuoles (black

490   arrows) in the cytoplasm of MSCs cultured in adipogenic media, confirming their differentiation

491   into adipocytes. *Right Panel:* Representative flow cytometry plots demonstrating the phenotype

492   of bone marrow derived MSCs as CD45$^-$CD34$^-$CD11b$^-$c-Kit$^-$CD31$^-$Sca-1$^+$CD29$^+$CD105$^+$ cells.

493   **B.** Representative flow cytometric histograms and bar chart demonstrating CD11b expression by

494   myeloid progenitors (MPs) cultured with or without MSCs with IFNγ stimulation for 72 hours.

495   **C.** Representative histograms of flow cytometric data and bar chart showing Ly6G expression by

496   myeloid progenitors (MPs) cultured with or without MSCs with IFNγ stimulation for 72 hours.

497   Results are representative of 3 independent experiments. Myeloid progenitors were isolated from

498   a pool of 5-6 animals in each experiment. P values are calculated using student's *t-test* and data

499   is represented as mean ± SEM. *p< 0.0001.

500 **Figure 3. MSCs inhibit differentiation of myeloid progenitors in a contact-dependent**

501 **manner**. **A.** Representative flow cytometric histograms and bar chart demonstrating CD11b

502 expression by myeloid progenitors (MPs) cultured with MSCs either in direct contact or using a

503 transwell chamber system, which separated MSCs from MPs, in the presence of IFNγ for 72

504 hours. Results are representative of 3 independent experiments. Myeloid progenitors were

505 isolated from a pool of 5-6 animals in each experiment. **B.** Real-time PCR analysis of PD-L1,

506 VTCN-1, CD200 and Ceacam-1 mRNA expression levels by resting MSCs. **C.** Real-time PCR

507 analysis of CD200 expression on resting and IFNγ-stimulated MSCs. Representative flow

508 cytometric histograms demonstrating expression of **D.** CD200 on MSCs, and **E.** CD200R1 on

509 myeloid progenitor cells. **F.** Representative flow cytometric histograms and bar chart showing

510 CD11b expression levels in myeloid progenitors cultured with control-shRNA (shCON) or

511 CD200-shRNA (shCD200) MSCs with IFNγ stimulation for 72 hours. Results are representative

512 of 3 independent experiments. Myeloid progenitors were isolated from a pool of 5-6 animals in

513 each experiment. P values are calculated using student's *t-test* and data is represented as mean ±

514 SEM. *p< 0.01, ** p< 0.001

515   **Figure 4. MSCs suppress ocular inflammation through expansion of myeloid progenitor**

516   **cells in a CD200-dependent manner. A.** Representative flow cytometric plots demonstrating

517     $CD34^+CD14^+CD11b^-$ myeloid progenitor in the cornea. **B.** Confocal microscopy image (×20) of

518   corneal whole mount confirming the presence of $CD14^+$ $CD11b^-$ cells in the peripheral corneal

519   stroma <mark>(Green: CD14, Red: CD11b)</mark>. **C.** Schematic representation of sterile injury induction in

520   mouse and experiment timeline. Corneal epithelium and anterior stroma are mechanically

521   removed using Algerbrush II. **D.** Bar chart demonstrating the frequencies of infiltrating corneal

522     $CD45^+$ cells in naïve mouse, injured mice without systemic MSC treatment, control-shRNA

523   (shCON) MSC-treated and CD200-shRNA (shCD200) MSC-treated mice. **E.** Representative

524   flow cytometric plots and bar chart demonstrating the frequencies of myeloid progenitors in

525   naïve cornea, injured cornea, injured cornea with IV administration of control-shRNA-treated

526   MSCs, and injured cornea with IV administration of CD200-shRNA-treated MSCs 48 hours after

527   injury induction. **F.** H &E staining of corneal cross-sections (×20) from naïve, untreated, control-

528   shRNA MSC-treated and CD200-shRNA MSC-treated mice demonstrating epithelial and

529   stromal layers and inflammatory cell infiltration. **G.** Real-time PCR analysis of relative

530   expression of IL-1β mRNA in naïve mice, injured mice without systemic MSC treatment,

531   control-shRNA MSC-treated and CD200-shRNA MSC-treated mice. Results are representative

532   of 2 independent experiments. Each group consisted of 4-5 animals in each experiment. P values

533   are calculated using student's *t-test* and data is represented as mean ± SEM. * $p < 0.05$, ** $p<$

534   0.01, *** $p< 0.001$
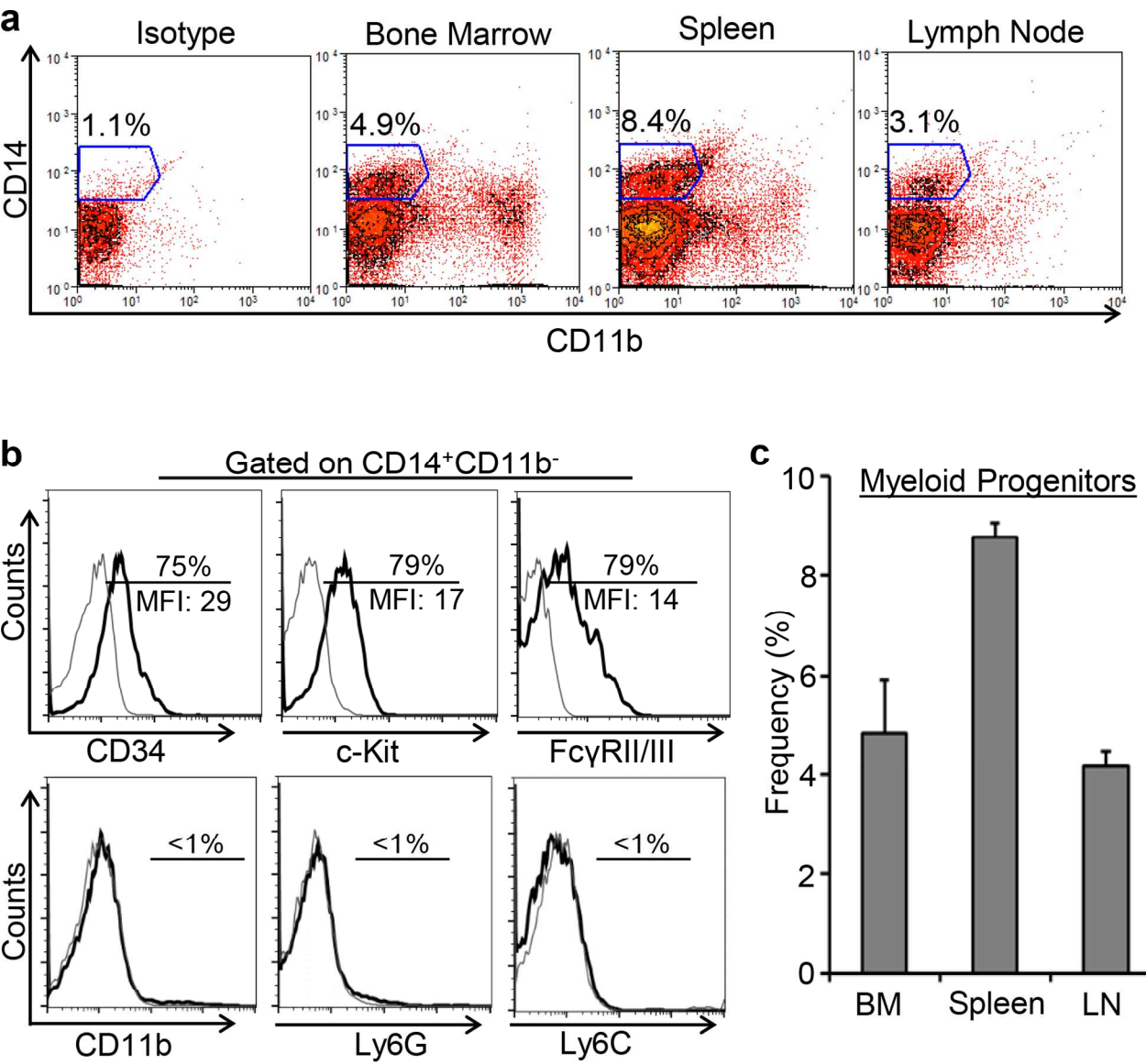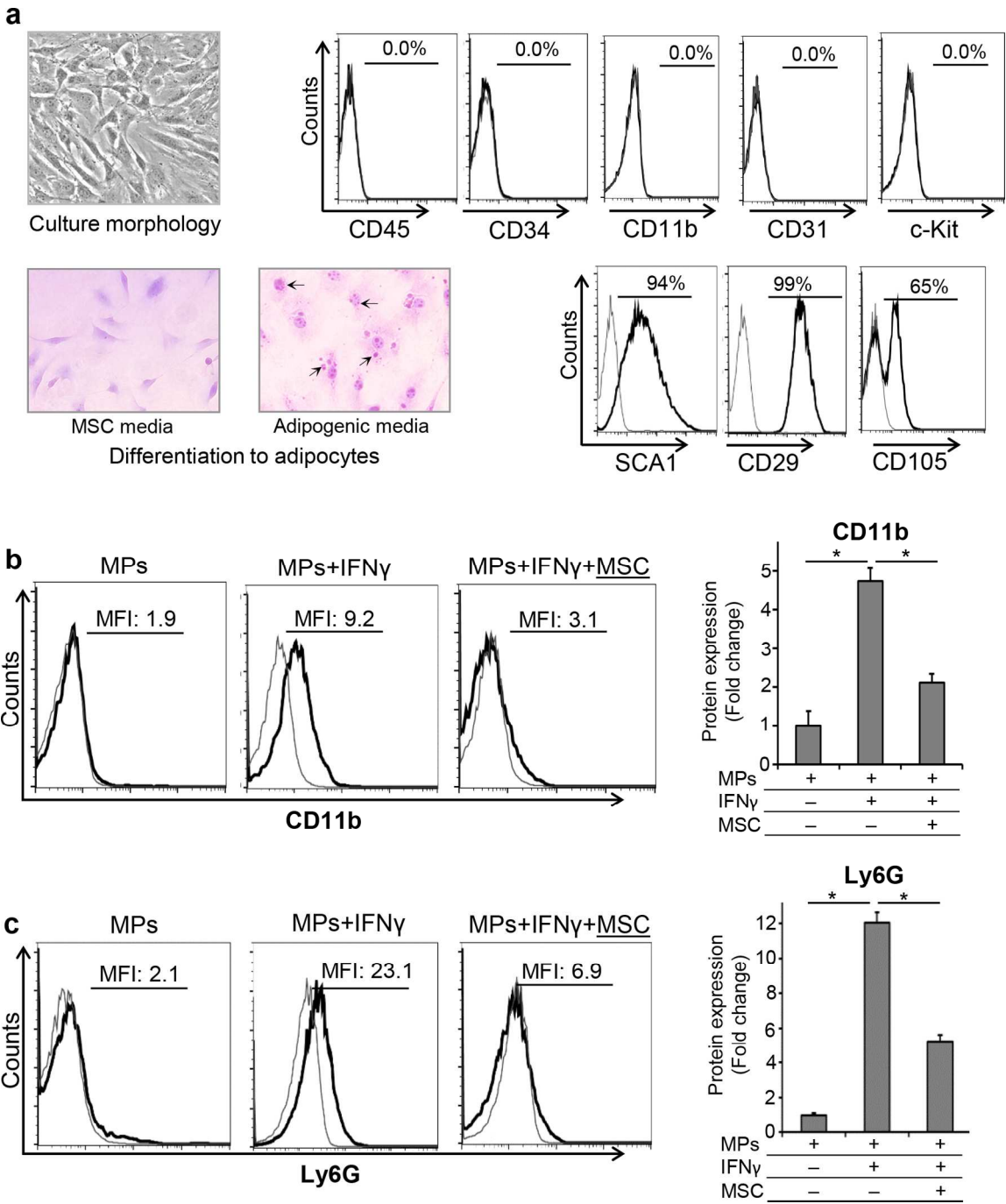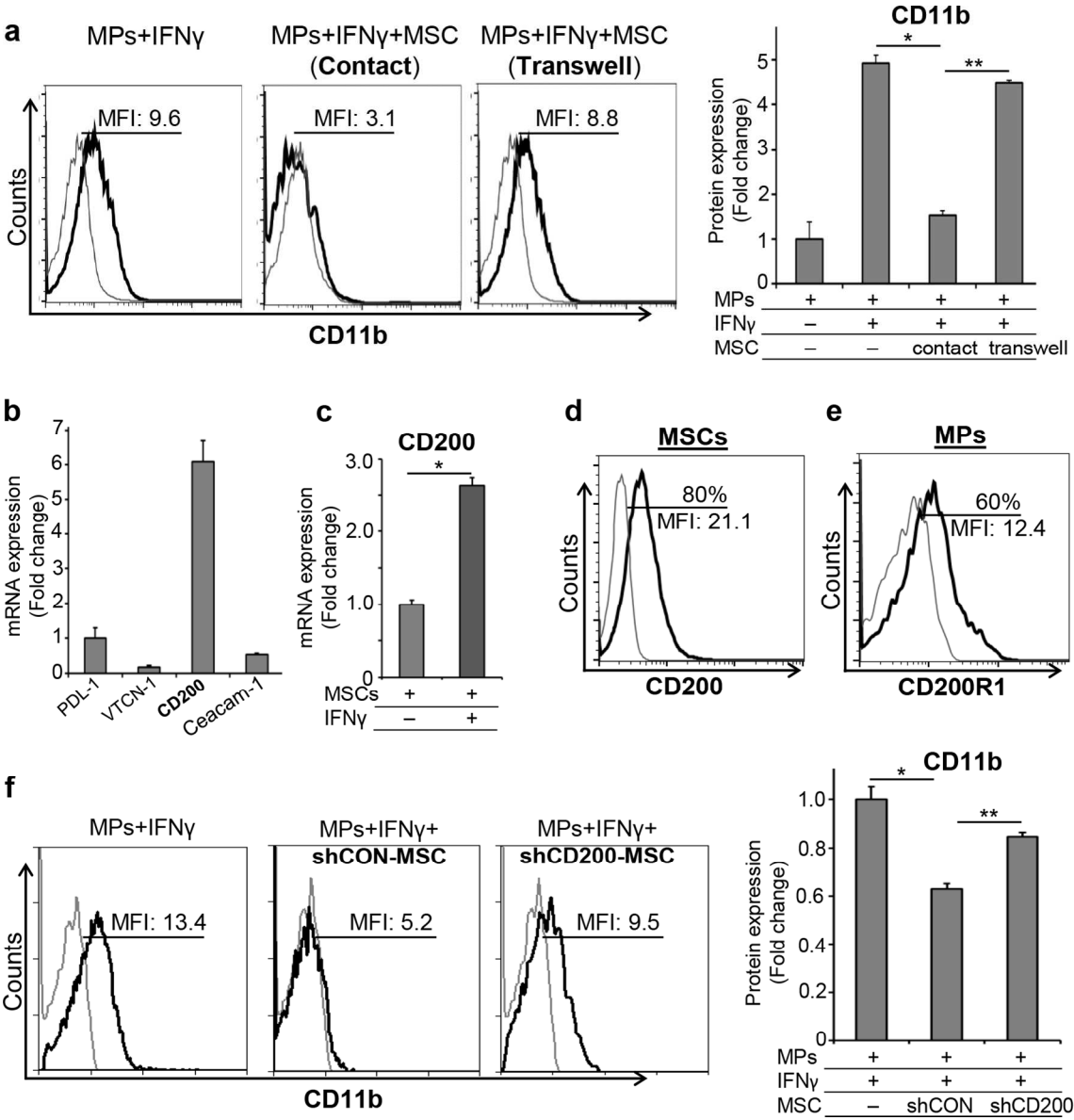
Figure 1.

a
Isotype | Bone Marrow | Spleen | Lymph Node
1.1% | 4.9% | 8.4% | 3.1%
CD14 (y-axis)
CD11b (x-axis)

b
Gated on CD14$^+$CD11b$^-$

Counts (y-axis)
75% MFI: 29 — CD34
79% MFI: 17 — c-Kit
79% MFI: 14 — FcγRII/III

Counts (y-axis)
<1% — CD11b
<1% — Ly6G
<1% — Ly6C

c
Myeloid Progenitors
Frequency (%)
BM | Spleen | LN

Figure 2.

a

Culture morphology

CD45 0.0% CD34 0.0% CD11b 0.0% CD31 0.0% c-Kit 0.0%

MSC media   Adipogenic media

Differentiation to adipocytes

SCA1 94% CD29 99% CD105 65%

b

MPs — MFI: 1.9

MPs+IFNγ — MFI: 9.2

MPs+IFNγ+MSC — MFI: 3.1

CD11b

CD11b

MPs	+	+	+
IFNγ	−	+	+
MSC	−	−	+

c

MPs — MFI: 2.1

MPs+IFNγ — MFI: 23.1

MPs+IFNγ+MSC — MFI: 6.9

Ly6G

Ly6G

MPs	+	+	+
IFNγ	−	+	+
MSC	−	−	+

Figure 3.

Figure 4.

SUPPLEMENTAL DATA
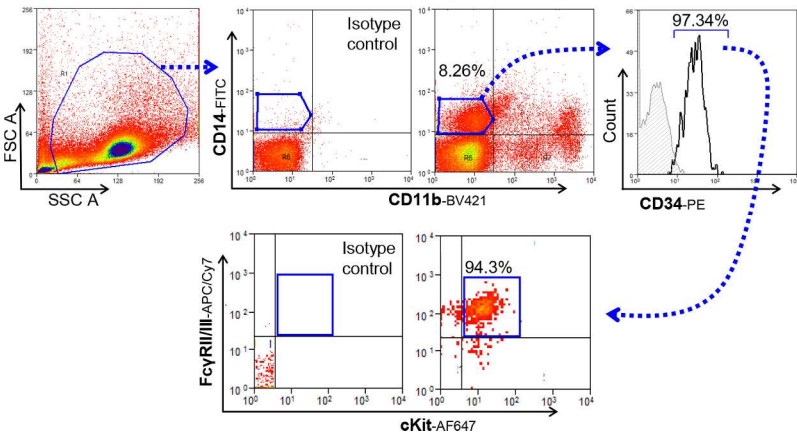
Figure S1. Myeloid progenitor cell characterization. Representative flow cytometry plots demonstrating the gating strategy for characterization of myeloid progenitors as $CD34^+CD14^+$c-$Kit^+Fc\gamma RII/III^+CD11b^-$ cells.
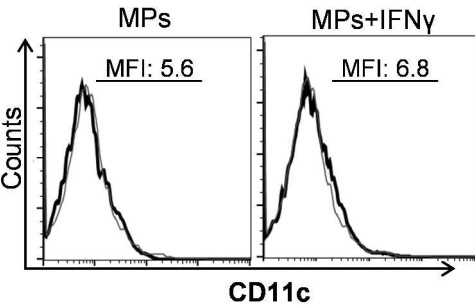

Figure S2. Myeloid progenitor cells do not differentiate into dendritic cells in the inflammatory environment. Isolated myeloid progenitors were stimulated with 100 ng/mL of IFNγ for 72 hours and acquisition of dendritic cell marker CD11c was evaluated using flow cytometry. Flow cytometric histograms demonstrate that myeloid progenitors do not express CD11c in the steady state or after stimulation with IFNγ.
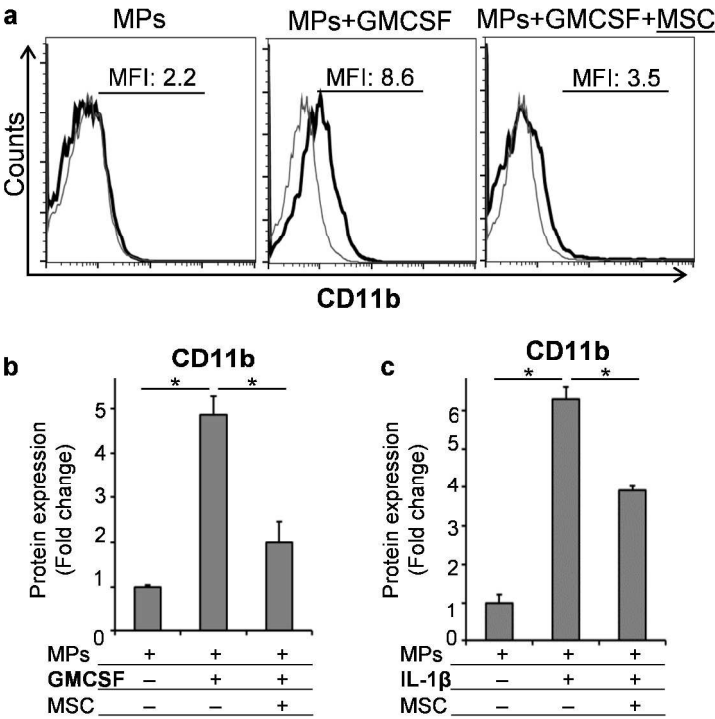
Figure S3. MSCs inhibit differentiation of myeloid progenitors stimulated with IL-1β or GMCSF. Myeloid progenitors were cultured with or without in vitro-expanded MSCs in the presence of (**a,b**) 10 ng/mL GMCSF or (**c**) 100 ng/mL IL-1β. As demonstrated in flow cytometric histograms and bar charts, myeloid progenitors express CD11b once stimulated with IL-1β or GMCSF, and MSCs suppress acquisition of CD11b by both IL-1β-treated and GMCSF-treated myeloid progenitors.
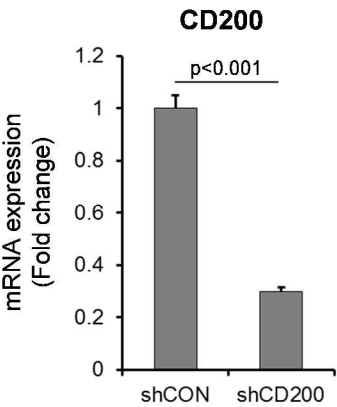

Figure S4. Knockdown efficiency of CD200-specific shRNA. MSCs were transfected with CD200-specific or non-specific control shRNA. CD200-specific shRNA suppressed endogenous expression of CD200 in MSCs by 70% 48 hours after transfection.

32

Contralateral   Injured

DAPI + GFP

Figure S5. MSCs home specifically to the injured cornea. Confocal microscopy image (×40) of corneal whole mounts demonstrating the presence of systematically administered green fluorescent protein (GFP)-positive MSCs in the injured cornea, but not in the contralateral cornea 48 hours after induction of injury.
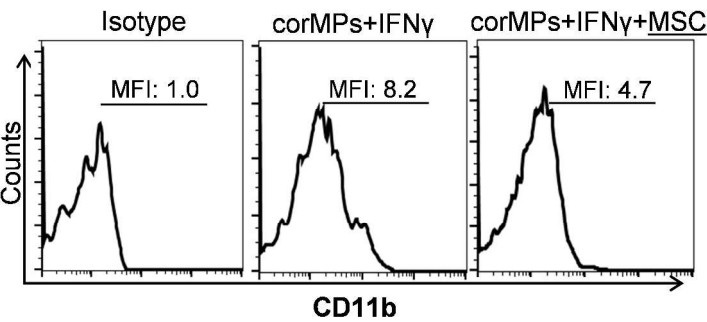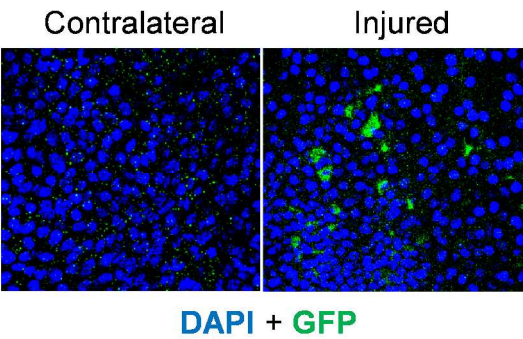
.

Isotype   corMPs+IFNγ   corMPs+IFNγ+MSC

MFI: 1.0   MFI: 8.2   MFI: 4.7

Counts

CD11b

Figure S6. MSCs inhibit acquisition of CD11b by corneal myeloid progenitors in vitro. Isolated corneal myeloid progenitors (corMPs) were cultured with or without in vitro-expanded MSCs in the presence of 100 ng/mL IFNγ for 72 hours. As demonstrated in flow cytometric histograms, once stimulated with IFNγ, corneal myeloid progenitors express CD11b. However, MSCs inhibit acquisition of CD11b differentiation marker by IFNγ-treated corneal myeloid progenitors.